Title: Granularity screening identifies candidate genes involved in vaccinia virus induced LC3 lipidation

Authors: Melanie Krause[1]*, Artur Yakimovich[1,2]*, Noemi Vágó[3], Ingo Drexler[3], Jason Mercer[1,4]

Affiliations:
[1] MRC Laboratory for Molecular Cell Biology, University College London, London, UK.
[2] Center for Advanced Systems Understanding (CASUS), Görlitz, Germany
[3] Institute for Virology, Düsseldorf University Hospital, Heinrich-Heine-University, Düsseldorf, Germany
[4] Institute of Microbiology and Infection, School of Biosciences, University of Birmingham, Birmingham, UK.
* Co-Corresponding Authors

Correspondence should be addressed to:

melanie.krause.15@alumni.ucl.ac.uk & a.yakimovich@hzdr.de

Abstract:

Autophagy is a catabolic process used for the degradation of organelles and proteins. Macroautophagy involves the formation of autophagosomes and subsequent fusion with lysosomes to mediate cargo degradation. It also functions as a cellular defence mechanism, known as xenophagy, during infection. Previous studies show that different viruses manipulate the autophagy pathway of the host cell to assure successful replication and/or virion assembly. Vaccinia virus (VACV), the prototypic poxvirus, replicates exclusively in the cytoplasm of host cells. It is known that VACV infection causes LC3 lipidation and prevents autophagosome formation, yet the double membrane vesicles formed during autophagy do not serve as the source of the mature VACV membrane. To date the viral protein(s) causing increased LC3 lipidation have not been identified. Here we developed an image-based screening approach based on LC3 granularity to identify candidate VACV genes affecting its lipidation. We identify several candidate viral membrane proteins as effectors of LC3 lipidation, suggesting that the interplay between VACV and autophagy is more directed than previously thought.

Introduction:

Vaccinia virus (VACV) is a double stranded DNA virus that replicates exclusively in the cytoplasm of its host cell. It was used as vaccine agent to successfully eradicate smallpox. However, in 2022 a closely related virus – monkeypox (mpox) caused a global outbreak with 91,000 confirmed human cases in 115 countries(Lansiaux et al., 2022; Moss, 2024). With a mortality rate of up to 15%, understanding the biology of mpox and other clinically relevant pox viruses continues to be crucial for treating human disease(Gessain et al., 2022). Additionally, VACV and several VACV derived poxvirus strains are used as vehicles for immunotherapy in cancer research and vaccine delivery. This necessitates continued research to further understand the interactions between VACV, its host and cellular immune responses.

An important part of the cellular immune response to pathogens residing in the cytoplasm, such as VACV, is autophagy. Macroautophagy (hereafter referred to as autophagy) provides protective immunity by capturing pathogens in autophagosomal compartments which later fuse with lysosomes to mediate the degradation of pathogens and other unwanted cytoplasmic content(Vargas et al., 2023).

ATG8 (in yeast) and ATG8-family proteins (in mammals) are crucial for functional autophagy. In mammals, at least seven ATG8 orthologs exist. The most studied ATG8 ortholog is LC3b (hereafter LC3), which is critical for the execution of autophagy and often used as a marker for autophagic activity and flux (Klionsky et al., 2021).

Two essential ubiquitin-like conjugation systems drive autophagy to covalently conjugate ATG8-family proteins to the phagophore membrane. The first complex crucial for this process is the ATG12-ATG5-ATG16L1 complex. The carboxy-terminal glycine of the small ubiquitin-like protein ATG12 is activated by transient linkage first to the E1-like enzyme ATG7 and then to the E2-like enzyme ATG10, before becoming covalently attached to ATG5(Mizushima et al., 1998; Tanida et al., 2001). This ATG12-ATG5 complex non-covalently associates with the protein ATG16L, forming the ATG12-ATG5-ATG16L1 complex that participates in the second ubiquitin-like conjugation reaction(Dooley et al., 2014). The second conjugation step results in the covalent addition of the lipid phosphatidylethanolamine (PE) to LC3. This process, known as ATG8/LC3 lipidation, is mediated by the E1-like ATG7 and E2-like ATG3 enzymes. The carboxy-terminal amino acids of LC3 are cleaved by the cysteine protease ATG4 presenting a conserved glycine residue. Cleaved LC3 can then be transiently linked to ATG7, then to ATG3, and finally to phosphatidylethanolamine (PE). The role of an E3-like ligase is filled by the ATG12-ATG5-ATG16 complex(Feng et al., 2014).

Although a complete lack of autophagosome formation is found in in VACV-infected cells, previous research showed that VACV infection leads to LC3 lipidation independent of the presence of ATG5 or ATG7(Moloughney et al., 2011). While ATG5 and ATG7 independent autophagy exists, and has been shown to mediate autophagic degradation of Shigella in intestinal cells(Ra et al., 2016), it does not typically involve LC3 lipidation(Arakawa et al., 2017; Nishida et al., 2009). Mologhney *et al*., also observed that VACV infection causes ATG12-ATG3 conjugation in the absence of ATG5 and ATG7, and that these ATG12-ATG3 conjugates cluster with viral DNA(Moloughney et al., 2011). They proposed a model whereby ATG12-ATG3 complexes drive aberrant LC3 lipidation due to spatial dislocation from the phagophore, resulting in a failure of autophagosome formation. The viral protein causing this complex formation has not been identified.

In this work, we set out to identify candidate viral genes involved in increased LC3 lipidation employing an image-based siRNA screen of 80 early VACV genes. To quantify $LC3^{+}$ autophagosomes, we used a readout based on single-cell granularity(Carpenter et al., 2006; Luc Vincent, 2000, 1992). The core methodology involves a pipeline starting with cell nuclei and cytoplasm segmentation(Carpenter et al., 2006), followed by single-cell granularity analysis(Luc Vincent, 2000, 1992) employing dsRed-LC3

63 fluorescence. We identified five VACV genes that up regulate and nine genes that down regulate LC3
64 lipidation. Conformational siRNA depletion coupled with immunoblot analysis for LC3 lipidation
65 showed that H3, A14, L5 and E8 influence LC3 lipidation during infection. This study delivers the first
66 systematic analysis of VACV genes intersecting with LC3 lipidation and provides the starting point for
67 detailed follow-up analysis of VACV mediated modulation of LC3 lipidation.

68 **Results:**

69 VACV infection leads to the accumulation of $LC3^+$ puncta

70 To confirm the previous finding that VACV induces LC3 lipidation, we monitored a 24 hr infection time
71 course. VACV infection led to the accumulation of $LC3^+$ puncta indicative of an enrichment of
72 autophagosomes. We observed a slight increase in $LC3^+$ puncta during VACV infection. While at late
73 time points post infection viral DNA replication sites appeared to show some minor overlap with
74 cytoplasmic LC3, we did not observe direct co-localization between LC3 and newly formed virions.
75 Interestingly accumulation of $LC3^+$ puncta occurred very early in infection and was already visible at
76 1 hpi (**Figure 1a**).

77 VACV infection causes increased LC3 lipidation

78 Moloughney *et al.* described an increase in LC3-II during VACV infection at 24 hpi assuming an increase
79 in lipidated LC3(Moloughney et al., 2011). To validate these findings and determine the flux of LC3
80 lipidation, we performed an infection kinetics assay with subsequent western blot analysis.
81 BafilomycinA1- and Torin1-treated samples were used as positive controls and 3-MA treated samples
82 as a negative control for LC3 lipidation. Consistent with Moloughney *et al.,* LC3-II was increased in
83 VACV infected cells. Quantification showed the increase to occur gradually over time with 5-fold more
84 14 kDa LC3 being present in cells 24 hpi compared to uninfected control samples (**Figure 1b**).

85 However, when visualizing LC3 protein using western blotting, two bands at 16 kDA and 14 kDa can
86 be observed. These bands are indicative of three different states of LC3: pro-LC3, LC3-I and LC3-II. To
87 be lipidated, pro-LC3 (14 kDA) is converted to LC3-I (16 kDa) through cleavage of carboxy-terminal
88 amino acids by ATG4. PE is then linked to the 16kDa LC3-I converting it into LC3-II (14 kDa). As pro-LC3
89 and LC3-II both migrate at 14 kDa by western blot, an increase in 14 kDa LC3 can be attributed to
90 either an increase in LC3-II formation or accumulation of pro-LC3 caused by a block in cleavage.

91 To differentiate between pro-LC3 and LC3-II during VACV infection, we utilized a Phospholipase D
92 (PLD) assay(Agrotis et al., 2019). This assay relies on the ability of PLD to cleave LC3-II, but not pro-
93 LC3. Incubating cell lysate with PLD shifts LC3-II from 14 kDa to 16 kDa, while pro-LC3 remains
94 unaffected. PLD-cleaved LC3 cannot be lipidated again due to the different cleavage sites of ATG4b
95 and PLD, thus a shift of LC3 from 14kDa to 16kDa in presence of PLD indicates that the increased
96 14kDA LC3 is due to LC3-II formation.

97 The PLD cleavage assay was performed at two different time points to differentiate between a pro-
98 cleavage block and LC3-II formation during both early and late stages of VACV infection. The earliest
99 time point with an increase in lower band LC3 sufficient for visualization was at 8 hpi. While 24 hpi
100 was chosen as the late time point representing the peak of VACV-mediated LC3 modification in WB-
101 based time course experiments. While incubation at 37 °C led to some degradation of LC3, enough
102 remained to be used as functional readout. ATG4b which cleaves both LC3-II and pro-LC3 was used as
103 positive control. An additional control used in this assay was uninfected lysate treated with
104 BafilomycinA1 and Torin1 which causes LC3-II resulting in a band shift to LC3-I upon PLD incubation.
105 Importantly, PLD treatment of either VACV infected or BafilomycinA1 + Torin1 treated samples
106 displayed an LC3 band shift with the lower band shifting upward, indicating that the lower LC3 band
107 mainly consists of LC3-II. This was documented for both time points at 8 and 24 hpi during VACV
108 infection (**Figure 2a&b**). This shows that VACV causes LC3 lipidation throughout the course of infection
109 rather than blocking pro-LC3 cleavage.

110 One or more early VACV genes facilitate LC3 lipidation

111 To narrow down the search for the viral gene(s) initiating LC3-II formation, we looked at VACV-induced
112 LC3 lipidation in the presence of three drugs known to interfere with the VACV life cycle. Cells were
113 infected with WT VACV (MOI 3) in the presence or absence of cycloheximide (CHX; 50 µM), MG-132
114 (25 µM), or Cytosine arabinoside (AraC; 10 µM), all of which are used in VACV research for temporal
115 inhibition of the VACV life cycle at distinct stages. CHX prevents early viral protein synthesis without
116 impacting virus entry and core release. MG132 prevents viral uncoating through proteasome
117 inhibition, while allowing for viral early gene expression(Kilcher et al., 2014; Satheshkumar et al., 2009;
118 Schmidt et al., 2013). AraC allows for uncoating and early gene expression, but blocks intermediate
119 and late gene expression by interfering with viral DNA synthesis(Furth and Cohen, 1968).

120 HeLa cells were infected with VACV WR WT, treated with CHX, MG132 or AraC, and LC3-II formation
121 was analysed by WB. MG132 and AraC did not prevent LC3 lipidation during infection. CHX however,

122 completely abrogated LC3-II formation suggesting an early viral gene product was responsible
123 (Figure 2c).

124 Assessing LC3-II lipidation during VACV infection using a dsRed-LC3-GFP marker cell line

125 While flow cytometry provides information regarding intensity and cell granularity, an image-based
126 read-out can provide additional single cell information including the number, size, and shape of LC3
127 puncta and, thus, is a preferable readout. To visualize the formation of $LC3^+$ autophagosomes, we
128 constructed a modified dsRed-LC3-I-GFP HeLa cell line expressing fluorescent LC3 generated using a
129 pQCXI-Puro-dsRed-LC3-GFP construct(Sheen et al., 2011) which is a modified version of another LC3
130 construct(Kabeya et al., 2000).

131 Here, LC3 bears a n-terminal dsRed tag and a c-terminal eGFP tag. As mentioned, during LC3
132 processing the c-terminus is modified by ATG4 cleaving the protein at the location indicated in
133 Figure 3a leading to removal of the GFP tag. This cleavage process is necessary to attach PE to LC3 and
134 to conjugate it to the autophagosome. Thus, LC3-II appears only as red, making it screen-able in both
135 IF and flow cytometry-based readout systems. Similar constructs have been published and used for
136 various applications in autophagy research such as to screen for autophagy inducing drugs with LC3
137 as readout for autophagic flux(Gump and Thorburn, 2014; Hundeshagen et al., 2011).

138 Cells were either treated with autophagy modulating drugs or infected with VACV. While only few red
139 autophagosomal puncta were present in untreated and uninfected cells, treatment with a
140 combination of BafilomycinA1 and Torin1 drastically increased the number of $LC3^+$ autophagosomes.
141 Additionally, we observed a steady increase in $LC3^+$ puncta during a time-course of VACV infection
142 peaking at 24 hpi (Figure 3b). These results confirmed that VACV infection induces LC3 lipidation, and
143 indicated that an image-based screening using this cell line as a readout for LC3-II formation is feasible.

144 To screen for the early viral gene(s) impacting LC3-II formation during VACV infection in the dsRed-
145 LC3-I-GFP HeLa cell line mentioned above, we utilized a VACV early gene siRNA library(Kilcher et al.,
146 2014) which targets 80 VACV early genes with three individual siRNAs per gene.

147 Development of a screening system measuring LC3-II granularity

148 The VACV early gene - LC3 lipidation screen was carried out by transfecting HeLa dsRed-LC3-I-GFP cells
149 with siRNAs directed against 80 early VACV genes(Caroline Martin et al. 2023; Kilcher et al., 2014).
150 Prior to infection cells were reverse transfected with siRNAs in 96-well plates and incubated for 16 hrs,

151 which is sufficient for early VACV gene depletion(Beerli et al., 2019; Kilcher et al., 2014; Valderrama
152 et al., 2006). Images were obtained using the Opera Phoenix High Content Screening System. Next,
153 image segmentation of individual cells was performed using a custom preprocessing script and a
154 CellProfiler pipeline(Carpenter et al., 2006).

155 Once individual cells were segmented, several single-cell readouts were tested such as the average
156 intensity of the dsRed signal, total intensity of dsRed signal, median intensity of dsRed signal and
157 granularity spectrum (see Methods). The latter was chosen as the readout as it most accurately
158 reflects the presence or absence of autophagosomes within the cell, with the granules indicating $LC3^{+}$
159 autophagosomes (**Figure 4a&b**). In this readout, the better the selected structuring element size fits
160 the signal, the higher the score. This makes it possible to detect the occurrence of larger granules in
161 the cytoplasm of the cell, upon adjustment of the structuring element size hyperparameter. Thus, this
162 is a single-cell level readout of granule formation. High granularity structures correspond to the
163 highest peak difference upon morphological opening with a structuring element of a fitting radius
164 (**Figure 4a&b**).

165 Identification of potential viral regulators of LC3 lipidation

166 For controls in this screen, we used untreated cells which were either infected (labelled as VACV) or
167 uninfected as well as cells treated with siScramble also either infected or uninfected. While siScramble
168 had no effect on LC3 granularity, VACV infection nearly doubled the granularity score both in presence
169 and absence of siScramble compared to uninfected cells (**Figure 4c**). The granularity score for VACV
170 treated with siScramble was slightly lower compared to untreated VACV infected cells. While we
171 expected to find that depletion of some VACV gene products would result in reduced LC3 puncta, we
172 also observed that depletion of some VACV early gene products led to an increased granularity score.
173 This suggests that VACV mediated LC3 lipidation is regulated in both directions.

174 Applying VACV untreated as threshold resulted in 53 screen hits with an increased and 27 screen hits
175 with a decreased LC3 granularity score. Applying VACV siScramble KD as control (indicated by the
176 dotted line in **Figure 4c**) results in 25 screen hits with increased LC3 granularity and 55 with decreased
177 LC3 granularity score.

178 Statistical analysis was carried out to decide which genes to select for follow-up experiments. For the
179 genes whose gene product depletion resulted in granularity increase, we selected the four highest
180 scoring genes A44L, B1L, A29L and H3L. Additionally A28L was selected based on the performance of

181 siRNA 1. For hits showing in decreased granularity, we selected the four lowest scoring genes A14L,
182 E8R, L5R and F11L. Additionally G5L was selected also based on the performance of siRNA 1.

183 VACV H3, G5, L5 and A14 may mediate VACV-induced LC3 lipidation

184 To validate the screening results and to confirm that the LC3 puncta seen in the screen correspond to
185 the LC3 lipidation results, the various candidate gene products were depleted using their respective
186 strongest performing siRNA. WB-based LC3 lipidation assays were carried out. Since cells were plated
187 at reduced confluency for siKD compared to other WB samples, the MOI was increased to six to
188 maintain the LC3 lipidation phenotype. The WB results indicated that H3 is the strongest candidate
189 for VACV-mediated negative regulation of LC3 lipidation. Depletion of H3 resulted in an even stronger
190 lipidation phenotype than siScramble with an increase of 25 % (**Figure 5a**).

191 In contrast, LC3 lipidation was significantly reduced upon siRNA mediated depletion of G5, L5 and A14
192 protein synthesis. A14 KD resulted in a reduction of LC3 lipidation by nearly 50 % when compared to
193 VACV infected siScramble samples. Interestingly, the uninfected siScramble control exhibits 60 % less
194 LC3 lipidation than VACV siScramble. Reduction of A14 therefore nearly abrogated the LC3 lipidation
195 phenotype of VACV compared to uninfected siScramble treated cells. Other gene products exposed
196 to siRNA mediated decay resulted in significant reduction of LC3 lipidation such as L5 (reduction of
197 lipidation by 45% compared to VACV siScramble) and G5 (reduction of lipidation by 33 % compared to
198 VACV siScramble) (**Figure 5b**).

199 To assure that the siRNA used in these assays could efficiently deplete the respective mRNA and
200 diminish the target protein synthesis, we used qRT-PCR to validate the KD efficiency of the siRNAs
201 (**Figure 5c**). All siRNAs showed some level of depletion of their respective target mRNAs to varying
202 degrees. An average reduction of mRNA transcripts for H3L, F11L and L5R was 30 %, while siRNAs for
203 A28L, B1R and E8R achieved a KD efficiency of 70 %. Thus, H3 depletion might have a stronger impact
204 on LC3 lipidation than suggested by **Figure 5a**, but limited siKD efficiency prevented manifestation of
205 the full phenotype in WB analysis. Likewise, the reduction of LC3 lipidation in siL5R and siA14L treated
206 samples might be more prominent if the KD efficiency was higher.

207 **Discussion:**

208 We have shown that VACV infection increased LC3 lipidation through one or more early gene
209 products. VACV causes an increase in LC3 lipidation rather than blocking the processing of pro-LC3.
210 The lipidation phenotype of LC3 manifests early during infection and increases over time resulting in

211 large amounts of lipidated LC3 at 24 hpi. We also discovered that this phenotype is caused by the
212 expression of VACV early gene(s). During the course of infection LC3 accumulates in punctae that could
213 potentially indicate fully formed autophagosomes, but might also be aggregates of LC3-II as previously
214 suggested(Moloughney et al., 2011).

215 Using a fluorescent dsRed-LC3-I-GFP cell line in an siRNA-based screen, we identified VACV early gene
216 candidates which were associated with the regulation of LC3 lipidation. The readout was based on
217 protein granularity. While the LC3 signal is specific to this screen, theoretically our approach could be
218 used to interrogate similar phenotypes such as endosomal structures or multivesicular bodies.
219 Therefore, we believe that this assay is applicable to other image-based screens and could be
220 employed in a multitude of high-content image-based screens.

221 We confirmed that siRNA mediated depletion of specific mRNAs derived from some early VACV
222 candidate genes changed the VACV LC3 lipidation phenotype. Further analysis will be necessary to
223 study these candidate gene products and their potential interaction with LC3 in more detail.

224 We are proposing three hypotheses regarding VACV and LC3 lipidation (**Figure 5d**): 1) LC3 lipidation
225 could be aberrant as suggested by Moloughney *et al*. This could be an autophagy evasion strategy by
226 the virus. As cargo is recruited into the forming autophagosome via autophagy receptors which bind
227 to LC3, aberrant LC3 lipidation would impede this process, leaving forming autophagosomes 'empty'.
228 2) Perhaps lipidated LC3 contributes to the formation of new virions. It was originally though that
229 VACV membranes may utilize autophagy machinery for membrane formation(Zhang et al., 2006).
230 While Beclin1, ATG5 and ATG7 have been ruled out by Zang et al., a role for lipidated LC3 has not been
231 addressed. 3) LC3 lipidation is a side effect of autophagy activation during infection. Upon sensing of
232 invading VACV virions the cell may initiate autophagosomal membrane formation to combat infection.
233 However, VACV-induced depletion of autophagy receptor proteins(Krause et al., 2024) results in
234 excess amounts of autophagosomal membranes.

235 While several siRNAs were initially found to cause an increase in LC3 puncta formation, follow up
236 experiments revealed only one siRNA that significantly upregulated LC3 lipidation upon infection. This
237 siRNA targeted the production of viral protein H3, which is a heparin sulphate binding protein on the
238 surface of IMVs. Some publications indicate that heparin prevents autophagy activation in mesangial
239 cells(Wang et al., 2014) and diabetes(Wang et al., 2015). In these studies, diabetic rats were treated
240 with heparin over an extended period which led to a reduction in LC3 levels and number of
241 autophagosomes. It is possible that H3 interactions with heparin during infection may increase the

242 effect the polysaccharide has on LC3, thus acting as a negative regulator of VACV-induced LC3
243 lipidation.

244 Amongst the candidate gene products to cause increased LC3 lipidation, confirmed through WB
245 analysis, were G5, L5, and A14. A14 is essential for viral membrane biogenesis and a major component
246 of the mature virion (MV) membrane. Together with A17 it forms viral membrane crescents which
247 progress into the immature virion (IV) membrane. A14 and A17 also form a lattice that is stabilized by
248 disulphide bonds which serves as an anchor within the viral membrane for other proteins important
249 for virion structure and morphogenesis(Betakova et al., 1999; Mercer and Traktman, 2003; Rodríguez
250 et al., 1998). G5 is thought to be a putative endonuclease required for double-strand break repair,
251 homologous recombination, and production of full-length viral genomic DNA(da Fonseca et al., 2004;
252 Moussatche and Condit, 2015; Senkevich et al., 2009). L5 is another viral membrane protein and part
253 of the entry fusion complex in VACV. Virions lacking L5 can bind to cells, but not enter the
254 cytoplasm(Laliberte et al., 2011; Townsley et al., 2005). E8 was another gene selected for WB based
255 validation. While E8 siKD did not lead to a significant decrease in VACV mediated LC3 lipidation by WB,
256 the characteristics of this protein still make it an interesting target for follow-up experiments. E8 is an
257 ER-localized membrane protein and ER stress is known to induce autophagy(Kawakami et al., 2009)
258 and to serve as a source of LC3 precursors(Ge et al., 2015).

259 Furthermore, studies on VACV suggest that soon after initial viral DNA synthesis, the replication sites
260 become entirely enwrapped by membranes of the ER which is essential for efficient VACV DNA
261 replication(Tolonen et al., 2001). Thus, initial VACV replication seemingly takes place near sites of
262 autophagosomal origin, further suggesting an option for disabling the autophagy pathway for
263 successful replication. We have previously shown that VACV utilizes ESCRT-mediated multi-vesicular
264 bodies during virion wrapping on intracellular enveloped viruses (IEVs)(Huttunen et al., 2021). The
265 formation of aberrant autophagosomal structures may be an additional source for wrapping
266 membranes for IEVs. Of the five proteins selected based on the screening results, three are membrane
267 proteins. This could be an indication for an involvement of LC3 in the formation of viral membranes.
268 Zhang *et al.*, showed that VACV membrane formation occurs independently of ATG5 and
269 Beclin1(Zhang et al., 2006). LC3 lipidation however also takes place in ATG5 and ATG7 deficient cells
270 during VACV infection(Moloughney et al., 2011). Moloughney *et al.*, suggested that the virus encodes
271 a viral protein that compensates for the lack of these proteins which are required for the E3 ligase
272 activity of the ATG12-ATG5-ATG16L complex that leads to conjugation of LC3 to PE on the
273 autophagosomal membrane. A recent pre-print suggested that VACV protein A52 prevents the
274 formation of autolysosomes by binding SNAP29, a protein that facilitates the fusion of

275 autophagosomes with lysosomes, which would provide an additional layer of autophagy pathway
276 modulation by VACV for autophagosomal escape (Niu et al., 2024).

277 In conjunction with previous literature, the findings described in this study suggest a closer interplay
278 of VACV with the host autophagy machinery than previously assumed. Deciphering the involvement
279 of these viral proteins in abrogating autophagy will be of interest for future research.

280 **Methods:**

281 Cell culture & Viruses

282 HeLa cells (WT as well as a HeLa based fluorescent cell line) were maintained in Dulbecco's Modified
283 Eagle Medium (DMEM, Life Technologies) supplemented with 10 % Foetal Bovine Serum (FBS, Life
284 Technologies), 1 mM sodium pyruvate (Thermo Fischer Scientific), 100 µM non-essential amino acids,
285 2 mM L-alanyl-L- glutamine dipeptide (GlutaMAX, ThermoFisher) and 1% Penicillin-Streptomycin (Life
286 Technologies) under at 37°C and 5 % CO_2. Cell lines were maintained in either T75 or T175 flasks and
287 passaged two to three times per week using Phosphate-buffered Saline (PBS) and Trypsin/EDTA (2.5g
288 Trypsin/litre, 0.2g EDTA/litre). The following viruses were used: Wild-type Western Reserve strain
289 (VACV WR WT) and VACV WR encoding an endogenous C-terminal mCherry tagged A4 core protein
290 (WR mCherry-A4)(Mercer and Helenius, 2008; Schmidt et al., 2013).

291 Reagents & Antibodies

292 Cytosine arabinoside (AraC) and cycloheximide (CHX) were obtained from Sigma-Aldrich, while
293 MG132 was purchased from MERCK Millipore. The drugs were used at 10 µM, 50 µM and 25 µM
294 respectively. DMSO (Sigma-Aldrich) was used to dissolve drugs and as negative control in all drug
295 related assays. Bafilomycin A1 from Streptomyces griseus (Sigma Aldrich) was used at 10 nM. Torin1
296 (MERCK Millipore) was used at 250 nM, 3-Methyladenine (3-MA) (Sigma Aldrich) was used at 5 mM.
297 The following antibodies were used: Anti-LC3b (CST #3868S) used in IF at 1:200 and in WB at 1:1000;
298 Anti-Tubulin (CST #9701S) used in WB at 1:5000. Hoechst Trihydrochloride Trihydrate 33342
299 (Invitrogen #H3570) was used for DNA staining in Immunofluorescence (IF) at 1:10,000. Secondary
300 antibodies were purchased from Invitrogen and LI-COR.

301 Imaging

302 For confocal imaging cells were seeded on 13 mm glass coverslips (VWR) at 60,000 cells per coverslip
303 the day prior to infection. Infection was carried out with WR mCh-A4 or WT virus at MOI 1 in DMEM,

304 and incubated for 1 hr at 37°C. The media was removed and replaced with full medium and incubated
305 for the desired time. Cells were fixed with 4 % FA-PBS for 15 mins. Cells were permeabilised with ice
306 cold MeOH at -20°C for 20 min, blocked with 3 % bovine serum albumin (BSA, from Sigma Aldrich) in
307 PBS for 1 hr, and stained with 30 µl primary antibody diluted in 3 % BSA-PBS for at least 1 hr at RT or
308 overnight at 4°C. The coverslips were washed three times for 5 mins in 3 % BSA-PBS before secondary
309 antibody and Hoechst staining for 1 hr at RT in 30 µl 3 % BSA- PBS and mounted on glass mounting
310 slides. Samples were imaged using a 63 x oil immersion objective (ACS APO) on a Leica TCS 2012 model
311 SPE confocal microscope. High content imaging was carried out as follows: Prior to image analysis cells
312 were fixed with 4 % FA. Antibody and Hoechst staining was carried out in a 40 µl volume on a shaker
313 using dilutions as stated above. The Opera Phenix High Content Screening System was used at 40 x
314 magnification with an air objective using 405 nm, 488 nm, 594 nm or 647 nm lasers and at least 15
315 images taken per well. CellProfiler was used to detect individual cells, based on Hoechst stained nuclei.

316 Infection time kinetics

317 For western blot or fractionation samples, HeLa cells were seeded in either 60 mm or 35 mm dishes
318 for confluency at infection. Infection was carried out in DMEM without FBS with VACV WR, or any
319 tagged virus, at MOI 3. Virus was incubated with the cells for 1 hr at 37°C, before aspirating and
320 replacing with full medium. Cells were either left untreated or treated with the indicated compounds
321 from the start of infection, and incubated at standard conditions. Samples were harvested at their
322 respective time points, by removing media and washing cells in PBS. Cells were harvested in lysis
323 buffer as indicated below.

324 PLD band shift assay

325 To determine the difference between lipidated LC3 and pro-LC3 on a western blot, a phospholipase D
326 (PLD) band shift assay was carried out following the previously published methodology(Agrotis et al.,
327 2019). The reaction was stopped by the addition of 3 x blue loading dye (CST #56036S) containing DTT
328 and immediately boiled at 95°C for 5 mins.

329 Western blot analysis

330 Cells were washed with cold PBS and subsequently scraped into 50 - 200 µl (depending on dish size)
331 lysis buffer containing protease inhibitor (#5872, NEB). The sample was then left on ice for at least
332 20 mins and subsequently spun down at 20,000 x *g* for 10 mins at 4°C. The supernatant was either
333 frozen and stored at -20°C or directly supplemented with 3 x blue loading dye containing DTT. Prior to

334 western blot analysis the samples were subject to 5 min incubation at 95°C. All protein samples were
335 loaded into 12 % Bis-Tris polyacrylamide gels and ran with MES SDS buffer (both Thermo Fisher
336 Scientific) at 60 Volt (V). Transfers were carried out onto 0.2 µm nitrocellulose membrane (Life
337 Technologies) using the semi-dry transfer system (both Biorad) at 10 V for 1 hr 15 mins, with transfer
338 buffer containing methanol (NuPAGE buffer, Thermo Fisher Scientific). Primary antibodies were
339 applied in 5 % BSA TBS-T over night at 4°C, then was washed three times in TBS-T. Membranes were
340 incubated with LiCor secondary antibodies for 1 hr at RT. Imaging of membranes was carried out with
341 using a LiCor Odyssey. Western blot quantifications were done using ImageJ (Version 2.0.0) with
342 tubulin used as a loading control where applicable.

343 qRT-PCR

344 Quantitative real-time PCR (qRT-PCR) was carried out to determine knock-down efficiency of early
345 VACV genes that were top hits in the LC3 lipidation screen. siRNA treated 33 mm dishes of HeLa cells
346 were infected with WT VACV at MOI 6 for 1 hr. Unbound virus was removed and replaced with full
347 medium. Cells were harvested at 24 hpi. RNA extraction, cDNA transcription and qRT-PCR were carried
348 out according to a recently published protocol(Huttunen and Mercer, 2019). Viral mRNA threshold
349 cycle (C_T) values were calculated and expression relative to and glyceraldehyde-3-phosphate
350 dehydrogenase (GAPDH) housekeeping gene determined. The qRT-PCR primers used are:

351 Table 1: List of qRT-PCR primers

Primer name	**Sequence (5'-3')**
E8R FWD Set 2	AAG GCT GGC GAC ATT TAG AG
E8R REV Set 2	GTG TGG GCG ATT ACC TTT CT
G5R FWD Set 3	GTA CAG ACC AGG TGG CTT AAA
G5R REV Set 3	CGG TAC ATT CAG CCT CGT T
L4R FWD Set 4	GAA CCT TAG CCG TTC AGA TGT A
L4R REV Set 4	TCT AAG GAG CAG GGA ACA ATT T
H3L FWD Set 4	GGA TAC TCA CGT GAA GGT CTT G
H3L REV Set 4	GAT TAT TCC AGT TGG GCT TGT TG
A28L FWD Set 5	ATG AGG CAA GGC GAG AAG
A28L REV Set 5	CAG TGG TAC GAC CTG ATA GAT G
A29L FWD Set 5	TCT ACC AGG AAG AAC TAG CAA ATC
A29L REV Set 5	CAA ACA GCA CAA CCA GTG TC
A44L FWD Set 5	TCG GGC AGA GGA AGT TCT AT
A44L REV Set 5	GCA CGA GGA TTT CTC AGA AGG
B1R FWD Set 3	GTT TCC GGA TCC TCT GAG TTT
B1R REV Set 3	GGA GAG TGT TGG AAT GAG TGT
F11L FWD Set 1	GAG GCT TCA TGC TGG GAT AC
F11L REV Set 1	GTA CCA CAG TCC TTG GAT TAC C
A14L FWD Set 2	GTT AGA CCA CAG CAG AGA AGT C
A14L REV Set 2	GGC ACG AGG GCT TTA ATA CT

GAPDH fw (RT-PCR, Ctrl)	AAG GTC GGA GTC AAC GGA TTT GGT
GAPDH rv (RT-PCR, Ctrl)	ACA AAG TGG TCG TTG AGG GCA ATG

352 siRNA-transfection

353 Lipofectamine RNAiMax (Thermo Fisher Scientific) was diluted 1 in 125 in pure DMEM for 5 minutes
354 at RT. siRNA dilutions and media containing Lipofectamine were then incubated together for a further
355 1 hr at RT. The AllStar Hs cell death control (Quiagen) was used as a control for transfection efficiency,
356 and AllStar negative (Quiagen) as an off-target, scrambled siRNA control. For western blot analysis
357 and confocal imaging, the siRNA-lipid complex mixture was then plated into a 30 mm dish. 300 000
358 HeLa cells were seeded on top of the mixture in 600 µl DMEM containing FBS.

359 For high content imaging of the siRNA LC3 screen a recently published protocol for high content
360 screening of VACV early genes(Caroline Martin et al., n.d.) was used. The primers used were previously
361 published(Kilcher et al., 2014).

362 Computational Analysis

363 The granularity spectrum measurement(Luc Vincent, 2000) used here is obtained through a
364 morphological opening operation(Luc Vincent, 1992) with disc structuring element of varying radius
365 to the cytoplasmic LC3 puncta observed in the cytoplasm of individual cells. The disc radius used for
366 the readout of all siRNA-treated cells was determined by comparing uninfected cells with infected
367 cells that had not been treated with siRNA.

368 Computational analysis of the image-based data has been performed using a combination of open-
369 source software and custom developed code. Image analysis was performed on a Desktop PC
370 equipped with Intel Core i7-8700K CPU at 3.7 GHz and 32 GB of RAM as well as GeForce 1080 Ti GPU.
371 Image analysis for the LC3 lipidation screen was performed using a custom pipeline for the CellProfiler
372 software(Carpenter et al., 2006) to detect LC3 granularity. Prior to granularity assessment the images
373 were processed for computational analysis: Images of cell nuclei were corrected for optical shading
374 and then convolved using a median filter. Next, the sum of all channel images was produced to obtain
375 a whole cytoplasm signal. Subsequently, processed nuclei and total images allowed for detection of
376 cell nuclei and cells as primary and secondary objects, respectively.

377 Based on the detected cells, LC3 signal granularity was measured for each single cell. To do so, a
378 morphological opening operation(Luc Vincent, 1992) with a disc structuring element of varying radius
379 was applied to the cytoplasmic LC3 puncta (594 nm channel) selected by the cytoplasm mask of

380 individual cells. The disc radius used for the readout of all siRNA-treated cells was determined by
381 comparing uninfected cells with infected cells that had not been treated with siRNA. The readout size
382 was selected based on comparisons of LC3 granularity between infected and uninfected HeLa cells.
383 The better the fit for the defined structuring element size, the higher the granularity score. To account
384 for variability of the granule size, the sum of all scores per cell was used as readout for LC3 granularity
385 on a single-cell level. CellProfiler outputs produced for each cell were then processed using a custom
386 KNIME-based workflow, normalizing and grouping the obtained measurements.

387 **Acknowledgements:**

388 We thank Robin Ketteler (MSB Medical School Berlin) and Alex Agrotis (University College London) for
389 reagents to perform the PLD band shift assay and helpful suggestions, Janos Kriston-Vizi (Laboratory
390 for Molecular Cell Biology, University College London) for help with imaging acquisition of high-
391 content screening data and Meserat Bogale (Laboratory for Molecular Cell Biology, University College
392 London) for facilitating data transfer.

393 This research was supported by MRC Laboratory for Molecular Cell Biology PhD program (M. Krause),
394 MRC Laboratory for Molecular Cell Biology at University College London (UCL) MC_UU_00012/7 (J.
395 Mercer) and the European Research Council 649101-UbiProPox (J. Mercer). AY was partially funded
396 by the Center for Advanced Systems Understanding (CASUS) which is financed by Germany's Federal
397 Ministry of Research, Technology and Space (BMFTR) and by the Saxon Ministry for Science, Culture,
398 and Tourism (SMWK) with tax funds on the basis of the budget approved by the Saxon State
399 Parliament. MW was supported by the Scultetus Early Career Fellowship Program at CASUS. AY
400 declares the following competing interest: role as an Editorial Board Member in mSphere. All other
401 authors declare no conflict of interest. All data is available from the corresponding authors upon
402 request.

403

404 **Figure Legends:**

405

406 **Figure 1: VACV infection causes an increase in LC3b puncta formation and in LC3-II.** A) HeLa
407 cells were infected with VACV for the time indicated and stained for LC3b or treated with 3-
408 MA, Bafilomycin and Torin1 at standard concentrations for 4 hrs. Representative images of
409 three biological replicates are shown. Scale bars represent 10µM. B) HeLa cells were infected
410 with VACV or incubated with BafilomycinA1 and Torin1 (B+T) or 3-MA for 8 hours. Right:

411 Quantification of four biological repeats of experiment shown. Statistical analysis: Unpaired
412 t-test with * P<0.05. Error bars represent SEM
413
414 **Figure 2: VACV infection causes LC3 lipidation, not pro-cleavage block through expression**
415 **of an early viral gene.** A) PLD assay carried out for VACV WR WT infection at 8 hpi with
416 BafilomycinA1 & Torin1 ctrl with quantification of n=3 biological replicates below. B) PLD
417 assay carried out for VACV WR WT infection at 24 hpi with BafilomycinA1 & Torin1 ctrl with
418 quantification of n=3 biological replicates below. C) HeLa cells were infected with VACV WR
419 WT at MOI30 for the time indicated in presence of 50 µM CHX, 25 µM MG132, 10 µM AraC
420 or DMSO with quantification of n=3 biological replicates on the right. Statistical analysis:
421 Unpaired t-test with * P<0.05 and **P<0.01. Error bars represent SEM.
422
423 **Figure 3: A cell line expressing a dsRed-LC3-I-GFP construct is used as readout for LC3**
424 **lipidation.**
425 A) Schematic representation of dsRed-LC3-I-GFP. B) Representative confocal images of the
426 cell line expressing the dsRed-LC3-I-GFP construct shown in A. HeLa cells were treated with
427 3-MA, Bafilomycin and/or Torin1 at standard concentrations for 4hrs or infected with VACV.
428 Scale bar indicates 15 µM.
429
430 **Figure 4: An early VACV gene siRNA screen identifies several candidates for VACV mediated**
431 **increase and decrease of LC3 puncta formation.** A&B) Principle approach to granularity
432 measurement. A Top: An example of a high-granularity cell. B Top: An example of a low-
433 granularity cell. Left-to-right channel merge, LC3 channel and morphologically processed LC3
434 micrograph using ray morphology open with a 10px circle as a structuring element. The yellow
435 dashed line corresponds to the position the linear profile was measured. A,B bottom: Line
436 profile intensity measurement of unprocessed (raw) and processed micrographs of high and
437 low granularity, highlighting the principle approach of granularity quantification. C) Cells were
438 treated with siRNA for 16 hrs and infected with WR WT at MOI 10. Red puncta of lipidated
439 LC3 were detected and used for granularity readout. Figure shows pooled results for all three
440 siRNAs per gene with each dot representing an n=3 for one specific siRNA. Error bars indicate
441 SEM. Scale bar indicates 10µm. Statistical analysis: Unpaired t-test with * P≤0.05, **P≤0.01
442 and ***P≤0.001

443

444 **Figure 5: Hit Validation of LC3 screen.** A) Validation of hits for LC3 lipidation decrease, sample
445 western blot (left) and quantification of three western blots (right). B) Validation of hits for
446 LC3 lipidation increase, sample western blot (left) and quantification of three western blots
447 (right). C) qRT-PCR validation of KD efficiency n=3 independent repeats in comparison to gene
448 expression in siScr samples. Statistical analysis of n=3 repeats for A and B: Unpaired T-test
449 with * $P<0.05$. All controls significant with at least *** $P<0.0001$. Absence of significance
450 indication in target genes means non-significant. Error bars represent SEM. **D Three different**
451 **models of LC3 lipidation:** 1) A viral protein causes ATG12–ATG3 conjugation. The ATG12–
452 ATG3 complex results in aberrant LC3 lipidation dislocated from phagophore leading to failure
453 in autophagosome formation. 2) Lipidated LC3 contributes to the formation of new virions.
454 3) LC3 lipidation is a side effect of autophagy activation during infection due to depletion of
455 autophagy receptor proteins.

References:

Agrotis, A., Pengo, N., Burden, J.J., Ketteler, R., 2019. Redundancy of human ATG4 protease isoforms in autophagy and LC3/GABARAP processing revealed in cells. Autophagy 15, 976–997. https://doi.org/10.1080/15548627.2019.1569925

Arakawa, S., Honda, S., Yamaguchi, H., Shimizu, S., 2017. Molecular mechanisms and physiological roles of Atg5/Atg7-independent alternative autophagy. Proc. Jpn. Acad. Ser. B Phys. Biol. Sci. 93, 378–385. https://doi.org/10.2183/pjab.93.023

Beerli, C., Yakimovich, A., Kilcher, S., Reynoso, G.V., Fläschner, G., Müller, D.J., Hickman, H.D., Mercer, J., 2019. Vaccinia virus hijacks EGFR signalling to enhance virus spread through rapid and directed infected cell motility. Nat. Microbiol. 4, 216–225. https://doi.org/10.1038/s41564-018-0288-2

Betakova, T., Wolffe, E.J., Moss, B., 1999. Regulation of vaccinia virus morphogenesis: phosphorylation of the A14L and A17L membrane proteins and C-terminal truncation of the A17L protein are dependent on the F10L kinase. J. Virol. 73, 3534–3543. https://doi.org/10.1128/JVI.73.5.3534-3543.1999

Caroline Martin, Samulel Kilcher, Jason Mercer, n.d. RNAi-Mediated Depletion of Poxvirus Proteins - Vaccinia Virus, 2019th ed, Methods in Molecular Biology. Humana Press.

Carpenter, A.E., Jones, T.R., Lamprecht, M.R., Clarke, C., Kang, I.H., Friman, O., Guertin, D.A., Chang, J.H., Lindquist, R.A., Moffat, J., Golland, P., Sabatini, D.M., 2006. CellProfiler: image analysis software for identifying and quantifying cell phenotypes. Genome Biol. 7, R100. https://doi.org/10.1186/gb-2006-7-10-r100

da Fonseca, F.G., Weisberg, A.S., Caeiro, M.F., Moss, B., 2004. Vaccinia virus mutants with alanine substitutions in the conserved G5R gene fail to initiate morphogenesis at the nonpermissive temperature. J. Virol. 78, 10238–10248. https://doi.org/10.1128/JVI.78.19.10238-10248.2004

Dooley, H.C., Razi, M., Polson, H.E.J., Girardin, S.E., Wilson, M.I., Tooze, S.A., 2014. WIPI2 Links LC3 Conjugation with PI3P, Autophagosome Formation, and Pathogen Clearance by Recruiting Atg12–5-16L1. Mol. Cell 55, 238–252. https://doi.org/10.1016/j.molcel.2014.05.021

Feng, Y., He, D., Yao, Z., Klionsky, D.J., 2014. The machinery of macroautophagy. Cell Res. 24, 24–41. https://doi.org/10.1038/cr.2013.168

Furth, J.J., Cohen, S.S., 1968. Inhibition of mammalian DNA polymerase by the 5'-triphosphate of 1-beta-d-arabinofuranosylcytosine and the 5'-triphosphate of 9-beta-d-arabinofuranoxyladenine. Cancer Res. 28, 2061–2067.

Ge, L., Wilz, L., Schekman, R., 2015. Biogenesis of autophagosomal precursors for LC3 lipidation from the ER-Golgi intermediate compartment. Autophagy 11, 2372–2374. https://doi.org/10.1080/15548627.2015.1105422

Gessain, A., Nakoune, E., Yazdanpanah, Y., 2022. Monkeypox. N. Engl. J. Med. 387, 1783–1793. https://doi.org/10.1056/NEJMra2208860

Gump, J.M., Thorburn, A., 2014. Sorting cells for basal and induced autophagic flux by quantitative ratiometric flow cytometry. Autophagy 10, 1327–1334. https://doi.org/10.4161/auto.29394

Hundeshagen, P., Hamacher-Brady, A., Eils, R., Brady, N.R., 2011. Concurrent detection of autolysosome formation and lysosomal degradation by flow cytometry in a high-content screen for inducers of autophagy. BMC Biol. 9, 38. https://doi.org/10.1186/1741-7007-9-38

Huttunen, M., Mercer, J., 2019. Quantitative PCR-Based Assessment of Vaccinia Virus RNA and DNA in Infected Cells. Methods Mol. Biol. Clifton NJ 2023, 189–208. https://doi.org/10.1007/978-1-4939-9593-6_12

Huttunen, M., Samolej, J., Evans, R.J., Yakimovich, A., White, I.J., Kriston-Vizi, J., Martin-Serrano, J., Sundquist, W.I., Frickel, E.-M., Mercer, J., 2021. Vaccinia virus hijacks ESCRT-mediated multivesicular body formation for virus egress. Life Sci. Alliance 4, e202000910. https://doi.org/10.26508/lsa.202000910

Kabeya, Y., Mizushima, N., Ueno, T., Yamamoto, A., Kirisako, T., Noda, T., Kominami, E., Ohsumi, Y., Yoshimori, T., 2000. LC3, a mammalian homologue of yeast Apg8p, is localized in autophagosome membranes after processing. EMBO J. 19, 5720–5728. https://doi.org/10.1093/emboj/19.21.5720

Kawakami, T., Inagi, R., Takano, H., Sato, S., Ingelfinger, J.R., Fujita, T., Nangaku, M., 2009. Endoplasmic reticulum stress induces autophagy in renal proximal tubular cells. Nephrol. Dial. Transplant. Off. Publ. Eur. Dial. Transpl. Assoc. - Eur. Ren. Assoc. 24, 2665–2672. https://doi.org/10.1093/ndt/gfp215

Kilcher, S., Schmidt, F.I., Schneider, C., Kopf, M., Helenius, A., Mercer, J., 2014. siRNA screen of early poxvirus genes identifies the AAA+ ATPase D5 as the virus genome-uncoating factor. Cell Host Microbe 15, 103–112. https://doi.org/10.1016/j.chom.2013.12.008

Klionsky, D.J., Abdel-Aziz, A.K., Abdelfatah, S., Abdellatif, M., Abdoli, A., Abel, S., Abeliovich, H., Abildgaard, M.H., Abudu, Y.P., Acevedo-Arozena, A., Adamopoulos, I.E., Adeli, K., Adolph, T.E., Adornetto, A.,

Aflaki, E., Agam, G., Agarwal, A., Aggarwal, B.B., Agnello, M., Agostinis, P., Agrewala, J.N., Agrotis, A., Aguilar, P.V., Ahmad, S.T., Ahmed, Z.M., Ahumada-Castro, U., Aits, S., Aizawa, S., Akkoc, Y., Akoumianaki, T., Akpinar, H.A., Al-Abd, A.M., Al-Akra, L., Al-Gharaibeh, A., Alaoui-Jamali, M.A., Alberti, S., Alcocer-Gómez, E., Alessandri, C., Ali, M., Alim Al-Bari, M.A., Aliwaini, S., Alizadeh, J., Almacellas, E., Almasan, A., Alonso, A., Alonso, G.D., Altan-Bonnet, N., Altieri, D.C., Álvarez, É.M.C., Alves, S., Alves Da Costa, C., Alzaharna, M.M., Amadio, M., Amantini, C., Amaral, C., Ambrosio, S., Amer, A.O., Ammanathan, V., An, Z., Andersen, S.U., Andrabi, S.A., Andrade-Silva, M., Andres, A.M., Angelini, S., Ann, D., Anozie, U.C., Ansari, M.Y., Antas, P., Antebi, A., Antón, Z., Anwar, T., Apetoh, L., Apostolova, N., Araki, T., Araki, Y., Arasaki, K., Araújo, W.L., Araya, J., Arden, C., Arévalo, M.-A., Arguelles, S., Arias, E., Arikkath, J., Arimoto, H., Ariosa, A.R., Armstrong-James, D., Arnauné-Pelloquin, L., Aroca, A., Arroyo, D.S., Arsov, I., Artero, R., Asaro, D.M.L., Aschner, M., Ashrafizadeh, M., Ashur-Fabian, O., Atanasov, A.G., Au, A.K., Auberger, P., Auner, H.W., Aurelian, L., Autelli, R., Avagliano, L., Ávalos, Y., Aveic, S., Aveleira, C.A., Avin-Wittenberg, T., Aydin, Y., Ayton, S., Ayyadevara, S., Azzopardi, M., Baba, M., Backer, J.M., Backues, S.K., Bae, D.-H., Bae, O.-N., Bae, S.H., Baehrecke, E.H., Baek, A., Baek, S.-H., Baek, S.H., Bagetta, G., Bagniewska-Zadworna, A., Bai, H., Bai, J., Bai, X., Bai, Y., Bairagi, N., Baksi, S., Balbi, T., Baldari, C.T., Balduini, W., Ballabio, A., Ballester, M., Balazadeh, S., Balzan, R., Bandopadhyay, R., Banerjee, Sreeparna, Banerjee, Sulagna, Bánréti, Á., Bao, Y., Baptista, M.S., Baracca, A., Barbati, C., Bargiela, A., Barilà, D., Barlow, P.G., Barmada, S.J., Barreiro, E., Barreto, G.E., Bartek, J., Bartel, B., Bartolome, A., Barve, G.R., Basagoudanavar, S.H., Bassham, D.C., Bast, R.C., Basu, A., Batoko, H., Batten, I., Baulieu, E.E., Baumgarner, B.L., Bayry, J., Beale, R., Beau, I., Beaumatin, F., Bechara, L.R.G., Beck, G.R., Beers, M.F., Begun, J., Behrends, C., Behrens, G.M.N., Bei, R., Bejarano, E., Bel, S., Behl, C., Belaid, A., Belgareh-Touzé, N., Bellarosa, C., Belleudi, F., Belló Pérez, M., Bello-Morales, R., Beltran, J.S.D.O., Beltran, S., Benbrook, D.M., Bendorius, M., Benitez, B.A., Benito-Cuesta, I., Bensalem, J., Berchtold, M.W., Berezowska, S., Bergamaschi, D., Bergami, M., Bergmann, A., Berliocchi, L., Berlioz-Torrent, C., Bernard, A., Berthoux, L., Besirli, C.G., Besteiro, S., Betin, V.M., Beyaert, R., Bezbradica, J.S., Bhaskar, K., Bhatia-Kissova, I., Bhattacharya, R., Bhattacharya, S., Bhattacharyya, S., Bhuiyan, Md.S., Bhutia, S.K., Bi, L., Bi, X., Biden, T.J., Bijian, K., Billes, V.A., Binart, N., Bincoletto, C., Birgisdottir, A.B., Bjorkoy, G., Blanco, G., Blas-Garcia, A., Blasiak, J., Blomgran, R., Blomgren, K., Blum, J.S., Boada-Romero, E., Boban, M., Boesze-Battaglia, K., Boeuf, P., Boland, B., Bomont, P., Bonaldo, P., Bonam, S.R., Bonfili, L., Bonifacino, J.S., Boone, B.A., Bootman, M.D., Bordi, M., Borner, C., Bornhauser, B.C., Borthakur, G., Bosch, J., Bose, S., Botana, L.M., Botas, J., Boulanger, C.M., Boulton, M.E., Bourdenx, M., Bourgeois, B., Bourke, N.M., Bousquet, G., Boya, P., Bozhkov, P.V., Bozi, L.H.M., Bozkurt, T.O., Brackney, D.E., Brandts, C.H., Braun, R.J., Braus, G.H., Bravo-Sagua, R., Bravo-San Pedro, J.M., Brest, P., Bringer, M.-A., Briones-Herrera, A., Broaddus, V.C., Brodersen, P., Brodsky, J.L., Brody, S.L., Bronson, P.G., Bronstein, J.M., Brown, C.N., Brown, R.E., Brum, P.C., Brumell, J.H., Brunetti-Pierri, N., Bruno, D., Bryson-Richardson, R.J., Bucci, C., Buchrieser, C., Bueno, M., Buitrago-Molina, L.E., Buraschi, S., Buch, S., Buchan, J.R., Buckingham, E.M., Budak, H., Budini, M., Bultynck, G., Burada, F., Burgoyne, J.R., Burón, M.I., Bustos, V., Büttner, S., Butturini, E., Byrd, A., Cabas, I., Cabrera-Benitez, S., Cadwell, K., Cai, J., Cai, L., Cai, Q., Cairó, M., Calbet, J.A., Caldwell, G.A., Caldwell, K.A., Call, J.A., Calvani, R., Calvo, A.C., Calvo-Rubio Barrera, M., Camara, N.O., Camonis, J.H., Camougrand, N., Campanella, M., Campbell, E.M., Campbell-Valois, F.-X., Campello, S., Campesi, I., Campos, J.C., Camuzard, O., Cancino, J., Candido De Almeida, D., Canesi, L., Caniggia, I., Canonico, B., Cantí, C., Cao, B., Caraglia, M., Caramés, B., Carchman, E.H., Cardenal-Muñoz, E., Cardenas, C., Cardenas, L., Cardoso, S.M., Carew, J.S., Carle, G.F., Carleton, G., Carloni, S., Carmona-Gutierrez, D., Carneiro, L.A., Carnevali, O., Carosi, J.M., Carra, S., Carrier, A., Carrier, L., Carroll, B., Carter, A.B., Carvalho, A.N., Casanova, M., Casas, C., Casas, J., Cassioli, C., Castillo, E.F., Castillo, K., Castillo-Lluva, S., Castoldi, F., Castori, M., Castro, A.F., Castro-Caldas, M., Castro-Hernandez, J., Castro-Obregon, S., Catz, S.D., Cavadas, C., Cavaliere, F., Cavallini, G., Cavinato, M., Cayuela, M.L., Cebollada Rica, P., Cecarini, V., Cecconi, F., Cechowska-Pasko, M., Cenci, S., Ceperuelo-Mallafré, V., Cerqueira, J.J., Cerutti, J.M., Cervia, D., Cetintas, V.B., Cetrullo, S., Chae, H.-J., Chagin, A.S., Chai, C.-Y., Chakrabarti, G., Chakrabarti, O., Chakraborty, Tapas, Chakraborty, Trinad, Chami, M., Chamilos, G., Chan, D.W., Chan, E.Y.W., Chan, E.D., Chan, H.Y.E., Chan, H.H., Chan, H., Chan, M.T.V., Chan, Y.S., Chandra, P.K., Chang, C.-P., Chang, C., Chang, H.-C., Chang, K., Chao, J., Chapman, T., Charlet-Berguerand, N., Chatterjee, S., Chaube, S.K., Chaudhary, A., Chauhan, S., Chaum, E., Checler, F., Cheetham, M.E., Chen, C.-S., Chen, G.-C., Chen, J.-F., Chen, L.L., Chen, Leilei, Chen, Lin, Chen, M., Chen, M.-K., Chen, N., Chen, Q., Chen, R.-H., Chen, S., Chen, Wei, Chen, Weiqiang, Chen, X.-M., Chen, X.-W., Chen, X., Chen, Yan, Chen, Y.-G., Chen, Yingyu, Chen, Yongqiang, Chen, Y.-J., Chen, Y.-Q., Chen, Z.S., Chen, Zhi, Chen, Z.-H., Chen, Z.J.,

Chen, Zhixiang, Cheng, H., Cheng, J., Cheng, S.-Y., Cheng, W., Cheng, X., Cheng, X.-T., Cheng, Y., Cheng, Z., Chen, Zhong, Cheong, H., Cheong, J.K., Chernyak, B.V., Cherry, S., Cheung, C.F.R., Cheung, C.H.A., Cheung, K.-H., Chevet, E., Chi, R.J., Chiang, A.K.S., Chiaradonna, F., Chiarelli, R., Chiariello, M., Chica, N., Chiocca, S., Chiong, M., Chiou, S.-H., Chiramel, A.I., Chiurchiù, V., Cho, D.-H., Choe, S.-K., Choi, A.M.K., Choi, M.E., Choudhury, K.R., Chow, N.S., Chu, C.T., Chua, J.P., Chua, J.J.E., Chung, H., Chung, K.P., Chung, S., Chung, S.-H., Chung, Y.-L., Cianfanelli, V., Ciechomska, I.A., Cifuentes, M., Cinque, L., Cirak, S., Cirone, M., Clague, M.J., Clarke, R., Clementi, E., Coccia, E.M., Codogno, P., Cohen, E., Cohen, M.M., Colasanti, T., Colasuonno, F., Colbert, R.A., Colell, A., Čolić, M., Coll, N.S., Collins, M.O., Colombo, M.I., Colón-Ramos, D.A., Combaret, L., Comincini, S., Cominetti, M.R., Consiglio, A., Conte, A., Conti, F., Contu, V.R., Cookson, M.R., Coombs, K.M., Coppens, I., Corasaniti, M.T., Corkery, D.P., Cordes, N., Cortese, K., Costa, M.D.C., Costantino, S., Costelli, P., Coto-Montes, A., Crack, P.J., Crespo, J.L., Criollo, A., Crippa, V., Cristofani, R., Csizmadia, T., Cuadrado, A., Cui, B., Cui, J., Cui, Yixian, Cui, Yong, Culetto, E., Cumino, A.C., Cybulsky, A.V., Czaja, M.J., Czuczwar, S.J., D'Adamo, S., D'Amelio, M., D'Arcangelo, D., D'Lugos, A.C., D'Orazi, G., Da Silva, J.A., Dafsari, H.S., Dagda, R.K., Dagdas, Y., Daglia, M., Dai, X., Dai, Yun, Dai, Yuyuan, Dal Col, J., Dalhaimer, P., Dalla Valle, L., Dallenga, T., Dalmasso, G., Damme, M., Dando, I., Dantuma, N.P., Darling, A.L., Das, H., Dasarathy, S., Dasari, S.K., Dash, S., Daumke, O., Dauphinee, A.N., Davies, J.S., Dávila, V.A., Davis, R.J., Davis, T., Dayalan Naidu, S., De Amicis, F., De Bosscher, K., De Felice, F., De Franceschi, L., De Leonibus, C., De Mattos Barbosa, M.G., De Meyer, G.R.Y., De Milito, A., De Nunzio, C., De Palma, C., De Santi, M., De Virgilio, C., De Zio, D., Debnath, J., DeBosch, B.J., Decuypere, J.-P., Deehan, M.A., Deflorian, G., DeGregori, J., Dehay, B., Del Rio, G., Delaney, J.R., Delbridge, L.M.D., Delorme-Axford, E., Delpino, M.V., Demarchi, F., Dembitz, V., Demers, N.D., Deng, H., Deng, Z., Dengjel, J., Dent, P., Denton, D., DePamphilis, M.L., Der, C.J., Deretic, V., Descoteaux, A., Devis, L., Devkota, S., Devuyst, O., Dewson, G., Dharmasivam, M., Dhiman, R., Di Bernardo, D., Di Cristina, M., Di Domenico, F., Di Fazio, P., Di Fonzo, A., Di Guardo, G., Di Guglielmo, G.M., Di Leo, L., Di Malta, C., Di Nardo, A., Di Rienzo, M., Di Sano, F., Diallinas, G., Diao, J., Diaz-Araya, G., Díaz-Laviada, I., Dickinson, J.M., Diederich, M., Dieudé, M., Dikic, I., Ding, S., Ding, W.-X., Dini, L., Dinić, J., Dinic, M., Dinkova-Kostova, A.T., Dionne, M.S., Distler, J.H.W., Diwan, A., Dixon, I.M.C., Djavaheri-Mergny, M., Dobrinski, I., Dobrovinskaya, O., Dobrowolski, R., Dobson, R.C.J., Đokić, J., Dokmeci Emre, S., Donadelli, M., Dong, B., Dong, X., Dong, Z., Dorn, G.W., Dotsch, V., Dou, H., Dou, J., Dowaidar, M., Dridi, S., Drucker, L., Du, A., Du, C., Du, G., Du, H.-N., Du, L.-L., Du Toit, A., Duan, S.-B., Duan, X., Duarte, S.P., Dubrovska, A., Dunlop, E.A., Dupont, N., Durán, R.V., Dwarakanath, B.S., Dyshlovoy, S.A., Ebrahimi-Fakhari, D., Eckhart, L., Edelstein, C.L., Efferth, T., Eftekharpour, E., Eichinger, L., Eid, N., Eisenberg, T., Eissa, N.T., Eissa, S., Ejarque, M., El Andaloussi, A., El-Hage, N., El-Naggar, S., Eleuteri, A.M., El-Shafey, E.S., Elgendy, M., Eliopoulos, A.G., Elizalde, M.M., Elks, P.M., Elsasser, H.-P., Elsherbiny, E.S., Emerling, B.M., Emre, N.C.T., Eng, C.H., Engedal, N., Engelbrecht, A.-M., Engelsen, A.S.T., Enserink, J.M., Escalante, R., Esclatine, A., Escobar-Henriques, M., Eskelinen, E.-L., Espert, L., Eusebio, M.-O., Fabrias, G., Fabrizi, C., Facchiano, A., Facchiano, F., Fadeel, B., Fader, C., Faesen, A.C., Fairlie, W.D., Falcó, A., Falkenburger, B.H., Fan, D., Fan, J., Fan, Y., Fang, E.F., Fang, Yanshan, Fang, Yognqi, Fanto, M., Farfel-Becker, T., Faure, M., Fazeli, G., Fedele, A.O., Feldman, A.M., Feng, D., Feng, J., Feng, L., Feng, Yibin, Feng, Yuchen, Feng, W., Fenz Araujo, T., Ferguson, T.A., Fernández, Á.F., Fernandez-Checa, J.C., Fernández-Veledo, S., Fernie, A.R., Ferrante, A.W., Ferraresi, A., Ferrari, M.F., Ferreira, J.C.B., Ferro-Novick, S., Figueras, A., Filadi, R., Filigheddu, N., Filippi-Chiela, E., Filomeni, G., Fimia, G.M., Fineschi, V., Finetti, F., Finkbeiner, S., Fisher, E.A., Fisher, P.B., Flamigni, F., Fliesler, S.J., Flo, T.H., Florance, I., Florey, O., Florio, T., Fodor, E., Follo, C., Fon, E.A., Forlino, A., Fornai, F., Fortini, P., Fracassi, A., Fraldi, A., Franco, B., Franco, R., Franconi, F., Frankel, L.B., Friedman, S.L., Fröhlich, L.F., Frühbeck, G., Fuentes, J.M., Fujiki, Y., Fujita, N., Fujiwara, Y., Fukuda, M., Fulda, S., Furic, L., Furuya, N., Fusco, C., Gack, M.U., Gaffke, L., Galadari, S., Galasso, A., Galindo, M.F., Gallolu Kankanamalage, S., Galluzzi, L., Galy, V., Gammoh, N., Gan, B., Ganley, I.G., Gao, F., Gao, H., Gao, M., Gao, P., Gao, S.-J., Gao, W., Gao, X., Garcera, A., Garcia, M.N., Garcia, V.E., García-Del Portillo, F., Garcia-Escudero, V., Garcia-Garcia, A., Garcia-Macia, M., García-Moreno, D., Garcia-Ruiz, C., García-Sanz, P., Garg, A.D., Gargini, R., Garofalo, T., Garry, R.F., Gassen, N.C., Gatica, D., Ge, L., Ge, W., Geiss-Friedlander, R., Gelfi, C., Genschik, P., Gentle, I.E., Gerbino, V., Gerhardt, C., Germain, K., Germain, M., Gewirtz, D.A., Ghasemipour Afshar, E., Ghavami, S., Ghigo, A., Ghosh, M., Giamas, G., Giampietri, C., Giatromanolaki, A., Gibson, G.E., Gibson, S.B., Ginet, V., Giniger, E., Giorgi, C., Girao, H., Girardin, S.E., Giridharan, M., Giuliano, S., Giulivi, C., Giuriato, S., Giustiniani, J., Gluschko, A., Goder, V., Goginashvili, A., Golab, J., Goldstone, D.C., Golebiewska, A., Gomes, L.R., Gomez, R., Gómez-Sánchez, R., Gomez-Puerto, M.C., Gomez-Sintes, R., Gong, Q., Goni, F.M., González-Gallego, J., Gonzalez-Hernandez, T.,

Gonzalez-Polo, R.A., Gonzalez-Reyes, J.A., González-Rodríguez, P., Goping, I.S., Gorbatyuk, M.S., Gorbunov, N.V., Görgülü, K., Gorojod, R.M., Gorski, S.M., Goruppi, S., Gotor, C., Gottlieb, R.A., Gozes, I., Gozuacik, D., Graef, M., Gräler, M.H., Granatiero, V., Grasso, D., Gray, J.P., Green, D.R., Greenhough, A., Gregory, S.L., Griffin, E.F., Grinstaff, M.W., Gros, F., Grose, C., Gross, A.S., Gruber, F., Grumati, P., Grune, T., Gu, X., Guan, J.-L., Guardia, C.M., Guda, K., Guerra, F., Guerri, C., Guha, P., Guillén, C., Gujar, S., Gukovskaya, A., Gukovsky, I., Gunst, J., Günther, A., Guntur, A.R., Guo, Chuanyong, Guo, Chun, Guo, H., Guo, L.-W., Guo, M., Gupta, P., Gupta, S.K., Gupta, S., Gupta, V.B., Gupta, V., Gustafsson, A.B., Gutterman, D.D., H.B., R., Haapasalo, A., Haber, J.E., Hać, A., Hadano, S., Hafrén, A.J., Haidar, M., Hall, B.S., Halldén, G., Hamacher-Brady, A., Hamann, A., Hamasaki, M., Han, W., Hansen, M., Hanson, P.I., Hao, Z., Harada, M., Harhaji-Trajkovic, L., Hariharan, N., Haroon, N., Harris, J., Hasegawa, T., Hasima Nagoor, N., Haspel, J.A., Haucke, V., Hawkins, W.D., Hay, B.A., Haynes, C.M., Hayrabedyan, S.B., Hays, T.S., He, C., He, Q., He, R.-R., He, Y.-W., He, Y.-Y., Heakal, Y., Heberle, A.M., Hejtmancik, J.F., Helgason, G.V., Henkel, V., Herb, M., Hergovich, A., Herman-Antosiewicz, A., Hernández, A., Hernandez, C., Hernandez-Diaz, S., Hernandez-Gea, V., Herpin, A., Herreros, J., Hervás, J.H., Hesselson, D., Hetz, C., Heussler, V.T., Higuchi, Y., Hilfiker, S., Hill, J.A., Hlavacek, W.S., Ho, E.A., Ho, I.H.T., Ho, P.W.-L., Ho, S.-L., Ho, W.Y., Hobbs, G.A., Hochstrasser, M., Hoet, P.H.M., Hofius, D., Hofman, P., Höhn, A., Holmberg, C.I., Hombrebueno, J.R., Yi-Ren Hong, C.-W.H., Hooper, L.V., Hoppe, T., Horos, R., Hoshida, Y., Hsin, I.-L., Hsu, H.-Y., Hu, B., Hu, D., Hu, L.-F., Hu, M.C., Hu, R., Hu, W., Hu, Y.-C., Hu, Z.-W., Hua, F., Hua, J., Hua, Y., Huan, C., Huang, Canhua, Huang, Chuanshu, Huang, Chuanxin, Huang, Chunling, Huang, H., Huang, K., Huang, M.L.H., Huang, R., Huang, S., Huang, T., Huang, X., Huang, Y.J., Huber, T.B., Hubert, V., Hubner, C.A., Hughes, S.M., Hughes, W.E., Humbert, M., Hummer, G., Hurley, J.H., Hussain, Sabah, Hussain, Salik, Hussey, P.J., Hutabarat, M., Hwang, H.-Y., Hwang, S., Ieni, A., Ikeda, F., Imagawa, Y., Imai, Y., Imbriano, C., Imoto, M., Inman, D.M., Inoki, K., Iovanna, J., Iozzo, R.V., Ippolito, G., Irazoqui, J.E., Iribarren, P., Ishaq, M., Ishikawa, M., Ishimwe, N., Isidoro, C., Ismail, N., Issazadeh-Navikas, S., Itakura, E., Ito, D., Ivankovic, D., Ivanova, S., Iyer, A.K.V., Izquierdo, J.M., Izumi, M., Jäättelä, M., Jabir, M.S., Jackson, W.T., Jacobo-Herrera, N., Jacomin, A.-C., Jacquin, E., Jadiya, P., Jaeschke, H., Jagannath, C., Jakobi, A.J., Jakobsson, J., Janji, B., Jansen-Dürr, P., Jansson, P.J., Jantsch, J., Januszewski, S., Jassey, A., Jean, S., Jeltsch-David, H., Jendelova, P., Jenny, A., Jensen, T.E., Jessen, N., Jewell, J.L., Ji, J., Jia, L., Jia, R., Jiang, L., Jiang, Q., Jiang, R., Jiang, T., Jiang, X., Jiang, Y., Jimenez-Sanchez, M., Jin, E.-J., Jin, F., Jin, H., Jin, Li, Jin, Luqi, Jin, M., Jin, S., Jo, E.-K., Joffre, C., Johansen, T., Johnson, G.V.W., Johnston, S.A., Jokitalo, E., Jolly, M.K., Joosten, L.A.B., Jordan, J., Joseph, B., Ju, D., Ju, J.-S., Ju, J., Juárez, E., Judith, D., Juhász, G., Jun, Y., Jung, C.H., Jung, S.-C., Jung, Y.K., Jungbluth, H., Jungverdorben, J., Just, S., Kaarniranta, K., Kaasik, A., Kabuta, T., Kaganovich, D., Kahana, A., Kain, R., Kajimura, S., Kalamvoki, M., Kalia, M., Kalinowski, D.S., Kaludercic, N., Kalvari, I., Kaminska, J., Kaminskyy, V.O., Kanamori, H., Kanasaki, K., Kang, C., Kang, R., Kang, S.S., Kaniyappan, S., Kanki, T., Kanneganti, T.-D., Kanthasamy, A.G., Kanthasamy, A., Kantorow, M., Kapuy, O., Karamouzis, M.V., Karim, Md.R., Karmakar, P., Katare, R.G., Kato, M., Kaufmann, S.H.E., Kauppinen, A., Kaushal, G.P., Kaushik, S., Kawasaki, K., Kazan, K., Ke, P.-Y., Keating, D.J., Keber, U., Kehrl, J.H., Keller, K.E., Keller, C.W., Kemper, J.K., Kenific, C.M., Kepp, O., Kermorgant, S., Kern, A., Ketteler, R., Keulers, T.G., Khalfin, B., Khalil, H., Khambu, B., Khan, S.Y., Khandelwal, V.K.M., Khandia, R., Kho, W., Khobrekar, N.V., Khuansuwan, S., Khundadze, M., Killackey, S.A., Kim, D., Kim, D.R., Kim, D.-H., Kim, D.-E., Kim, E.Y., Kim, E.-K., Kim, H.-R., Kim, H.-S., Hyung-Ryong Kim, Kim, Jeong Hun, Kim, J.K., Kim, J.-H., Kim, J., Kim, Ju Hwan, Kim, K.I., Kim, P.K., Kim, S.-J., Kimball, S.R., Kimchi, A., Kimmelman, A.C., Kimura, T., King, M.A., Kinghorn, K.J., Kinsey, C.G., Kirkin, V., Kirshenbaum, L.A., Kiselev, S.L., Kishi, S., Kitamoto, K., Kitaoka, Y., Kitazato, K., Kitsis, R.N., Kittler, J.T., Kjaerulff, O., Klein, P.S., Klopstock, T., Klucken, J., Knævelsrud, H., Knorr, R.L., Ko, B.C.B., Ko, F., Ko, J.-L., Kobayashi, H., Kobayashi, S., Koch, I., Koch, J.C., Koenig, U., Kögel, D., Koh, Y.H., Koike, M., Kohlwein, S.D., Kocaturk, N.M., Komatsu, M., König, J., Kono, T., Kopp, B.T., Korcsmaros, T., Korkmaz, G., Korolchuk, V.I., Korsnes, M.S., Koskela, A., Kota, J., Kotake, Y., Kotler, M.L., Kou, Y., Koukourakis, M.I., Koustas, E., Kovacs, A.L., Kovács, T., Koya, D., Kozako, T., Kraft, C., Krainc, D., Krämer, H., Krasnodembskaya, A.D., Kretz-Remy, C., Kroemer, G., Ktistakis, N.T., Kuchitsu, K., Kuenen, S., Kuerschner, L., Kukar, T., Kumar, Ajay, Kumar, Ashok, Kumar, Deepak, Kumar, Dhiraj, Kumar, S., Kume, S., Kumsta, C., Kundu, C.N., Kundu, M., Kunnumakkara, A.B., Kurgan, L., Kutateladze, T.G., Kutlu, O., Kwak, S., Kwon, H.J., Kwon, T.K., Kwon, Y.T., Kyrmizi, I., La Spada, A., Labonté, P., Ladoire, S., Laface, I., Lafont, F., Lagace, D.C., Lahiri, V., Lai, Z., Laird, A.S., Lakkaraju, A., Lamark, T., Lan, S.-H., Landajuela, A., Lane, D.J.R., Lane, J.D., Lang, C.H., Lange, C., Langel, Ü., Langer, R., Lapaquette, P., Laporte, J., LaRusso, N.F., Lastres-Becker, I., Lau, W.C.Y., Laurie, G.W., Lavandero, S., Law, B.Y.K., Law, H.K., Layfield, R., Le, W., Le Stunff, H., Leary, A.Y., Lebrun, J.-J.,

Leck, L.Y.W., Leduc-Gaudet, J.-P., Lee, C., Lee, C.-P., Lee, D.-H., Lee, E.B., Lee, E.F., Lee, G.M., Lee, H.-J., Lee, H.K., Lee, J.M., Lee, J.S., Lee, J.-A., Lee, J.-Y., Lee, J.H., Lee, M., Lee, M.G., Lee, M.J., Lee, M.-S., Lee, Sang Yoon, Lee, S.-J., Lee, Stella Y., Lee, S.B., Lee, W.H., Lee, Y.-R., Lee, Yong-ho, Lee, Youngil, Lefebvre, C., Legouis, R., Lei, Y.L., Lei, Y., Leikin, S., Leitinger, G., Lemus, L., Leng, S., Lenoir, O., Lenz, G., Lenz, H.J., Lenzi, P., León, Y., Leopoldino, A.M., Leschczyk, C., Leskelä, S., Letellier, E., Leung, C.-T., Leung, P.S., Leventhal, J.S., Levine, B., Lewis, P.A., Ley, K., Li, B., Li, D.-Q., Li, Jianming, Li, Jing, Li, Jiong, Li, K., Li, L., Li, Mei, Li, Min, Li, Min, Li, Ming, Li, Mingchuan, Li, P.-L., Li, M.-Q., Li, Q., Li, S., Li, T., Li, Wei, Li, Wenming, Li, X., Li, Y.-P., Li, Y., Li, Zhiqiang, Li, Zhiyong, Li, Zhiyuan, Lian, J., Liang, C., Liang, Q., Liang, W., Liang, Yongheng, Liang, YongTian, Liao, G., Liao, L., Liao, M., Liao, Y.-F., Librizzi, M., Lie, P.P.Y., Lilly, M.A., Lim, H.J., Lima, T.R.R., Limana, F., Lin, C., Lin, C.-W., Lin, D.-S., Lin, F.-C., Lin, J.D., Lin, K.M., Lin, K.-H., Lin, L.-T., Lin, P.-H., Lin, Q., Lin, S., Lin, S.-J., Lin, W., Lin, X., Lin, Y.-X., Lin, Y.-S., Linden, R., Lindner, P., Ling, S.-C., Lingor, P., Linnemann, A.K., Liou, Y.-C., Lipinski, M.M., Lipovšek, S., Lira, V.A., Lisiak, N., Liton, P.B., Liu, C., Liu, C.-H., Liu, C.-F., Liu, C.H., Liu, F., Liu, Hao, Liu, H.-S., Liu, Hua-feng, Liu, Huifang, Liu, Jia, Liu, Jing, Liu, Julia, Liu, Leyuan, Liu, Longhua, Liu, M., Liu, Q., Liu, Wei, Liu, Wende, Liu, X.-H., Liu, Xiaodong, Liu, Xingguo, Liu, Xu, Liu, Xuedong, Liu, Yanfen, Liu, Yang, Liu, Yang, Liu, Yueyang, Liu, Yule, Livingston, J.A., Lizard, G., Lizcano, J.M., Ljubojevic-Holzer, S., LLeonart, M.E., Llobet-Navàs, D., Llorente, A., Lo, C.H., Lobato-Márquez, D., Long, Q., Long, Y.C., Loos, B., Loos, J.A., López, M.G., López-Doménech, G., López-Guerrero, J.A., López-Jiménez, A.T., López-Pérez, Ó., López-Valero, I., Lorenowicz, M.J., Lorente, M., Lorincz, P., Lossi, L., Lotersztajn, S., Lovat, P.E., Lovell, J.F., Lovy, A., Lőw, P., Lu, G., Lu, H., Lu, J.-H., Lu, J.-J., Lu, M., Lu, S., Luciani, A., Lucocq, J.M., Ludovico, P., Luftig, M.A., Luhr, M., Luis-Ravelo, D., Lum, J.J., Luna-Dulcey, L., Lund, A.H., Lund, V.K., Lünemann, J.D., Lüningschrör, P., Luo, H., Luo, R., Luo, S., Luo, Z., Luparello, C., Lüscher, B., Luu, L., Lyakhovich, A., Lyamzaev, K.G., Lystad, A.H., Lytvynchuk, L., Ma, A.C., Ma, C., Ma, M., Ma, N.-F., Ma, Q.-H., Ma, X., Ma, Y., Ma, Z., MacDougald, O.A., Macian, F., MacIntosh, G.C., MacKeigan, J.P., Macleod, K.F., Maday, S., Madeo, F., Madesh, M., Madl, T., Madrigal-Matute, J., Maeda, A., Maejima, Y., Magarinos, M., Mahavadi, P., Maiani, E., Maiese, K., Maiti, P., Maiuri, M.C., Majello, B., Major, M.B., Makareeva, E., Malik, F., Mallilankaraman, K., Malorni, W., Maloyan, A., Mammadova, N., Man, G.C.W., Manai, F., Mancias, J.D., Mandelkow, E.-M., Mandell, M.A., Manfredi, A.A., Manjili, M.H., Manjithaya, R., Manque, P., Manshian, B.B., Manzano, R., Manzoni, C., Mao, K., Marchese, C., Marchetti, S., Marconi, A.M., Marcucci, F., Mardente, S., Mareninova, O.A., Margeta, M., Mari, M., Marinelli, S., Marinelli, O., Mariño, G., Mariotto, S., Marshall, R.S., Marten, M.R., Martens, S., Martin, A.P.J., Martin, K.R., Martin, Sara, Martin, Shaun, Martín-Segura, A., Martín-Acebes, M.A., Martin-Burriel, I., Martin-Rincon, M., Martin-Sanz, P., Martina, J.A., Martinet, W., Martinez, Aitor, Martinez, Ana, Martinez, J., Martinez Velazquez, M., Martinez-Lopez, N., Martinez-Vicente, M., Martins, D.O., Martins, J.O., Martins, W.K., Martins-Marques, T., Marzetti, E., Masaldan, S., Masclaux-Daubresse, C., Mashek, D.G., Massa, V., Massieu, L., Masson, G.R., Masuelli, L., Masyuk, A.I., Masyuk, T.V., Matarrese, P., Matheu, A., Matoba, S., Matsuzaki, S., Mattar, P., Matte, A., Mattoscio, D., Mauriz, J.L., Mauthe, M., Mauvezin, C., Maverakis, E., Maycotte, P., Mayer, J., Mazzoccoli, G., Mazzoni, C., Mazzulli, J.R., McCarty, N., McDonald, C., McGill, M.R., McKenna, S.L., McLaughlin, B., McLoughlin, F., McNiven, M.A., McWilliams, T.G., Mechta-Grigoriou, F., Medeiros, T.C., Medina, D.L., Megeney, L.A., Megyeri, K., Mehrpour, M., Mehta, J.L., Meijer, A.J., Meijer, A.H., Mejlvang, J., Meléndez, A., Melk, A., Memisoglu, G., Mendes, A.F., Meng, D., Meng, F., Meng, T., Menna-Barreto, R., Menon, M.B., Mercer, C., Mercier, A.E., Mergny, J.-L., Merighi, A., Merkley, S.D., Merla, G., Meske, V., Mestre, A.C., Metur, S.P., Meyer, C., Meyer, H., Mi, W., Mialet-Perez, J., Miao, J., Micale, L., Miki, Y., Milan, E., Milczarek, M., Miller, D.L., Miller, S.I., Miller, S., Millward, S.W., Milosevic, I., Minina, E.A., Mirzaei, H., Mirzaei, H.R., Mirzaei, M., Mishra, A., Mishra, N., Mishra, P.K., Misirkic Marjanovic, M., Misasi, R., Misra, A., Misso, G., Mitchell, C., Mitou, G., Miura, T., Miyamoto, S., Miyazaki, Makoto, Miyazaki, Mitsunori, Miyazaki, T., Miyazawa, K., Mizushima, N., Mogensen, T.H., Mograbi, B., Mohammadinejad, R., Mohamud, Y., Mohanty, A., Mohapatra, S., Möhlmann, T., Mohmmed, A., Moles, A., Moley, K.H., Molinari, M., Mollace, V., Møller, A.B., Mollereau, B., Mollinedo, F., Montagna, C., Monteiro, M.J., Montella, A., Montes, L.R., Montico, B., Mony, V.K., Monzio Compagnoni, G., Moore, M.N., Moosavi, M.A., Mora, A.L., Mora, M., Morales-Alamo, D., Moratalla, R., Moreira, P.I., Morelli, E., Moreno, S., Moreno-Blas, D., Moresi, V., Morga, B., Morgan, A.H., Morin, F., Morishita, H., Moritz, O.L., Moriyama, M., Moriyasu, Y., Morleo, M., Morselli, E., Moruno-Manchon, J.F., Moscat, J., Mostowy, S., Motori, E., Moura, A.F., Moustaid-Moussa, N., Mrakovcic, M., Muciño-Hernández, G., Mukherjee, A., Mukhopadhyay, S., Mulcahy Levy, J.M., Mulero, V., Muller, S., Münch, C., Munjal, A., Munoz-Canoves, P., Muñoz-Galdeano, T., Münz, C., Murakawa, T., Muratori, C., Murphy, B.M., Murphy, J.P., Murthy,

A., Myöhänen, T.T., Mysorekar, I.U., Mytych, J., Nabavi, S.M., Nabissi, M., Nagy, P., Nah, J., Nahimana, A., Nakagawa, I., Nakamura, K., Nakatogawa, H., Nandi, S.S., Nanjundan, M., Nanni, M., Napolitano, G., Nardacci, R., Narita, M., Nassif, M., Nathan, I., Natsumeda, M., Naude, R.J., Naumann, C., Naveiras, O., Navid, F., Nawrocki, S.T., Nazarko, T.Y., Nazio, F., Negoita, F., Neill, T., Neisch, A.L., Neri, L.M., Netea, M.G., Neubert, P., Neufeld, T.P., Neumann, D., Neutzner, A., Newton, P.T., Ney, P.A., Nezis, I.P., Ng, C.C.W., Ng, T.B., Nguyen, H.T.T., Nguyen, L.T., Ni, H.-M., Ní Cheallaigh, C., Ni, Z., Nicolao, M.C., Nicoli, F., Nieto-Diaz, M., Nilsson, P., Ning, S., Niranjan, R., Nishimune, H., Niso-Santano, M., Nixon, R.A., Nobili, A., Nobrega, C., Noda, T., Nogueira-Recalde, U., Nolan, T.M., Nombela, I., Novak, I., Novoa, B., Nozawa, T., Nukina, N., Nussbaum-Krammer, C., Nylandsted, J., O'Donovan, T.R., O'Leary, S.M., O'Rourke, E.J., O'Sullivan, M.P., O'Sullivan, T.E., Oddo, S., Oehme, I., Ogawa, M., Ogier-Denis, E., Ogmundsdottir, M.H., Ogretmen, B., Oh, G.T., Oh, S.-H., Oh, Y.J., Ohama, T., Ohashi, Y., Ohmuraya, M., Oikonomou, V., Ojha, R., Okamoto, K., Okazawa, H., Oku, M., Oliván, S., Oliveira, J.M.A., Ollmann, M., Olzmann, J.A., Omari, S., Omary, M.B., Önal, G., Ondrej, M., Ong, S.-B., Ong, S.-G., Onnis, A., Orellana, J.A., Orellana-Muñoz, S., Ortega-Villaizan, M.D.M., Ortiz-Gonzalez, X.R., Ortona, E., Osiewacz, H.D., Osman, A.-H.K., Osta, R., Otegui, M.S., Otsu, K., Ott, C., Ottobrini, L., Ou, J.J., Outeiro, T.F., Oynebraten, I., Ozturk, M., Pagès, G., Pahari, S., Pajares, M., Pajvani, U.B., Pal, R., Paladino, S., Pallet, N., Palmieri, M., Palmisano, G., Palumbo, C., Pampaloni, F., Pan, L., Pan, Q., Pan, W., Pan, X., Panasyuk, G., Pandey, R., Pandey, U.B., Pandya, V., Paneni, F., Pang, S.Y., Panzarini, E., Papademetrio, D.L., Papaleo, E., Papinski, D., Papp, D., Park, E.C., Park, H.T., Park, J.-M., Park, J.-I., Park, J.T., Park, J., Park, S.C., Park, S.-Y., Parola, A.H., Parys, J.B., Pasquier, A., Pasquier, B., Passos, J.F., Pastore, N., Patel, H.H., Patschan, D., Pattingre, S., Pedraza-Alva, G., Pedraza-Chaverri, J., Pedrozo, Z., Pei, G., Pei, J., Peled-Zehavi, H., Pellegrini, J.M., Pelletier, J., Peñalva, M.A., Peng, D., Peng, Y., Penna, F., Pennuto, M., Pentimalli, F., Pereira, C.M., Pereira, G.J.S., Pereira, L.C., Pereira De Almeida, L., Perera, N.D., Pérez-Lara, Á., Perez-Oliva, A.B., Pérez-Pérez, M.E., Periyasamy, P., Perl, A., Perrotta, C., Perrotta, I., Pestell, R.G., Petersen, M., Petrache, I., Petrovski, G., Pfirrmann, T., Pfister, A.S., Philips, J.A., Pi, H., Picca, A., Pickrell, A.M., Picot, S., Pierantoni, G.M., Pierdominici, M., Pierre, P., Pierrefite-Carle, V., Pierzynowska, K., Pietrocola, F., Pietruczuk, M., Pignata, C., Pimentel-Muiños, F.X., Pinar, M., Pinheiro, R.O., Pinkas-Kramarski, R., Pinton, P., Pircs, K., Piya, S., Pizzo, P., Plantinga, T.S., Platta, H.W., Plaza-Zabala, A., Plomann, M., Plotnikov, E.Y., Plun-Favreau, H., Pluta, R., Pocock, R., Pöggeler, S., Pohl, C., Poirot, M., Poletti, A., Ponpuak, M., Popelka, H., Popova, B., Porta, H., Porte Alcon, S., Portilla-Fernandez, E., Post, M., Potts, M.B., Poulton, J., Powers, T., Prahlad, V., Prajsnar, T.K., Praticò, D., Prencipe, R., Priault, M., Proikas-Cezanne, T., Promponas, V.J., Proud, C.G., Puertollano, R., Puglielli, L., Pulinilkunnil, T., Puri, D., Puri, R., Puyal, J., Qi, X., Qi, Y., Qian, W., Qiang, L., Qiu, Y., Quadrilatero, J., Quarleri, J., Raben, N., Rabinowich, H., Ragona, D., Ragusa, M.J., Rahimi, N., Rahmati, M., Raia, V., Raimundo, N., Rajasekaran, N.-S., Ramachandra Rao, S., Rami, A., Ramírez-Pardo, I., Ramsden, D.B., Randow, F., Rangarajan, P.N., Ranieri, D., Rao, H., Rao, L., Rao, R., Rathore, S., Ratnayaka, J.A., Ratovitski, E.A., Ravanan, P., Ravegnini, G., Ray, S.K., Razani, B., Rebecca, V., Reggiori, F., Régnier-Vigouroux, A., Reichert, A.S., Reigada, D., Reiling, J.H., Rein, T., Reipert, S., Rekha, R.S., Ren, H., Ren, J., Ren, W., Renault, T., Renga, G., Reue, K., Rewitz, K., Ribeiro De Andrade Ramos, B., Riazuddin, S.A., Ribeiro-Rodrigues, T.M., Ricci, J.-E., Ricci, R., Riccio, V., Richardson, D.R., Rikihisa, Y., Risbud, M.V., Risueño, R.M., Ritis, K., Rizza, S., Rizzuto, R., Roberts, H.C., Roberts, L.D., Robinson, K.J., Roccheri, M.C., Rocchi, S., Rodney, G.G., Rodrigues, T., Rodrigues Silva, V.R., Rodriguez, A., Rodriguez-Barrueco, R., Rodriguez-Henche, N., Rodriguez-Rocha, H., Roelofs, J., Rogers, R.S., Rogov, V.V., Rojo, A.I., Rolka, K., Romanello, V., Romani, L., Romano, A., Romano, P.S., Romeo-Guitart, D., Romero, L.C., Romero, M., Roney, J.C., Rongo, C., Roperto, S., Rosenfeldt, M.T., Rosenstiel, P., Rosenwald, A.G., Roth, K.A., Roth, L., Roth, S., Rouschop, K.M.A., Roussel, B.D., Roux, S., Rovere-Querini, P., Roy, A., Rozieres, A., Ruano, D., Rubinsztein, D.C., Rubtsova, M.P., Ruckdeschel, K., Ruckenstuhl, C., Rudolf, E., Rudolf, R., Ruggieri, A., Ruparelia, A.A., Rusmini, P., Russell, R.R., Russo, G.L., Russo, M., Russo, R., Ryabaya, O.O., Ryan, K.M., Ryu, K.-Y., Sabater-Arcis, M., Sachdev, U., Sacher, M., Sachse, C., Sadhu, A., Sadoshima, J., Safren, N., Saftig, P., Sagona, A.P., Sahay, G., Sahebkar, A., Sahin, M., Sahin, O., Sahni, S., Saito, N., Saito, S., Saito, T., Sakai, R., Sakai, Y., Sakamaki, J.-I., Saksela, K., Salazar, G., Salazar-Degracia, A., Salekdeh, G.H., Saluja, A.K., Sampaio-Marques, B., Sanchez, M.C., Sanchez-Alcazar, J.A., Sanchez-Vera, V., Sancho-Shimizu, V., Sanderson, J.T., Sandri, M., Santaguida, S., Santambrogio, L., Santana, M.M., Santoni, G., Sanz, A., Sanz, P., Saran, S., Sardiello, M., Sargeant, T.J., Sarin, A., Sarkar, C., Sarkar, Sovan, Sarrias, M.-R., Sarkar, Surajit, Sarmah, D.T., Sarparanta, J., Sathyanarayan, A., Sathyanarayanan, R., Scaglione, K.M., Scatozza, F., Schaefer, L., Schafer, Z.T., Schaible, U.E., Schapira, A.H.V., Scharl, M., Schatzl, H.M., Schein, C.H., Scheper, W., Scheuring, D., Schiaffino, M.V., Schiappacassi, M., Schindl, R.,

Schlattner, U., Schmidt, O., Schmitt, R., Schmidt, S.D., Schmitz, I., Schmukler, E., Schneider, A., Schneider, B.E., Schober, R., Schoijet, A.C., Schott, M.B., Schramm, M., Schröder, B., Schuh, K., Schüller, C., Schulze, R.J., Schürmanns, L., Schwamborn, J.C., Schwarten, M., Scialo, F., Sciarretta, S., Scott, M.J., Scotto, K.W., Scovassi, A.I., Scrima, A., Scrivo, A., Sebastian, D., Sebti, S., Sedej, S., Segatori, L., Segev, N., Seglen, P.O., Seiliez, I., Seki, E., Selleck, S.B., Sellke, F.W., Selsby, J.T., Sendtner, M., Senturk, S., Seranova, E., Sergi, C., Serra-Moreno, R., Sesaki, H., Settembre, C., Setty, S.R.G., Sgarbi, G., Sha, O., Shacka, J.J., Shah, J.A., Shang, D., Shao, C., Shao, F., Sharbati, S., Sharkey, L.M., Sharma, D., Sharma, G., Sharma, K., Sharma, P., Sharma, S., Shen, H.-M., Shen, H., Shen, J., Shen, M., Shen, W., Shen, Z., Sheng, R., Sheng, Z., Sheng, Z.-H., Shi, J., Shi, X., Shi, Y.-H., Shiba-Fukushima, K., Shieh, J.-J., Shimada, Y., Shimizu, S., Shimozawa, M., Shintani, T., Shoemaker, C.J., Shojaei, S., Shoji, I., Shravage, B.V., Shridhar, V., Shu, C.-W., Shu, H.-B., Shui, K., Shukla, A.K., Shutt, T.E., Sica, V., Siddiqui, A., Sierra, A., Sierra-Torre, V., Signorelli, S., Sil, P., Silva, B.J.D.A., Silva, J.D., Silva-Pavez, E., Silvente-Poirot, S., Simmonds, R.E., Simon, A.K., Simon, H.-U., Simons, M., Singh, A., Singh, L.P., Singh, R., Singh, S.V., Singh, S.K., Singh, S.B., Singh, S., Singh, S.P., Sinha, D., Sinha, R.A., Sinha, S., Sirko, A., Sirohi, K., Sivridis, E.L., Skendros, P., Skirycz, A., Slaninová, I., Smaili, S.S., Smertenko, A., Smith, M.D., Soenen, S.J., Sohn, E.J., Sok, S.P.M., Solaini, G., Soldati, T., Soleimanpour, S.A., Soler, R.M., Solovchenko, A., Somarelli, J.A., Sonawane, A., Song, F., Song, H.K., Song, J.-X., Song, K., Song, Z., Soria, L.R., Sorice, M., Soukas, A.A., Soukup, S.-F., Sousa, D., Sousa, N., Spagnuolo, P.A., Spector, S.A., Srinivas Bharath, M.M., St. Clair, D., Stagni, V., Staiano, L., Stalnecker, C.A., Stankov, M.V., Stathopulos, P.B., Stefan, K., Stefan, S.M., Stefanis, L., Steffan, J.S., Steinkasserer, A., Stenmark, H., Sterneckert, J., Stevens, C., Stoka, V., Storch, S., Stork, B., Strappazzon, F., Strohecker, A.M., Stupack, D.G., Su, H., Su, L.-Y., Su, L., Suarez-Fontes, A.M., Subauste, C.S., Subbian, S., Subirada, P.V., Sudhandiran, G., Sue, C.M., Sui, X., Summers, C., Sun, G., Sun, J., Sun, K., Sun, M., Sun, Q., Sun, Y., Sun, Z., Sunahara, K.K.S., Sundberg, E., Susztak, K., Sutovsky, P., Suzuki, H., Sweeney, G., Symons, J.D., Sze, S.C.W., Szewczyk, N.J., Tabęcka-Łonczynska, A., Tabolacci, C., Tacke, F., Taegtmeyer, H., Tafani, M., Tagaya, M., Tai, H., Tait, S.W.G., Takahashi, Y., Takats, S., Talwar, P., Tam, C., Tam, S.Y., Tampellini, D., Tamura, A., Tan, C.T., Tan, E.-K., Tan, Y.-Q., Tanaka, Masaki, Tanaka, Motomasa, Tang, D., Tang, J., Tang, T.-S., Tanida, I., Tao, Z., Taouis, M., Tatenhorst, L., Tavernarakis, N., Taylor, A., Taylor, G.A., Taylor, J.M., Tchetina, E., Tee, A.R., Tegeder, I., Teis, D., Teixeira, N., Teixeira-Clerc, F., Tekirdag, K.A., Tencomnao, T., Tenreiro, S., Tepikin, A.V., Testillano, P.S., Tettamanti, G., Tharaux, P.-L., Thedieck, K., Thekkinghat, A.A., Thellung, S., Thinwa, J.W., Thirumalaikumar, V.P., Thomas, S.M., Thomes, P.G., Thorburn, A., Thukral, L., Thum, T., Thumm, M., Tian, L., Tichy, A., Till, A., Timmerman, V., Titorenko, V.I., Todi, S.V., Todorova, K., Toivonen, J.M., Tomaipitinca, L., Tomar, D., Tomas-Zapico, C., Tomić, S., Tong, B.C.-K., Tong, C., Tong, X., Tooze, S.A., Torgersen, M.L., Torii, S., Torres-López, L., Torriglia, A., Towers, C.G., Towns, R., Toyokuni, S., Trajkovic, V., Tramontano, D., Tran, Q.-G., Travassos, L.H., Trelford, C.B., Tremel, S., Triola, G., Trougakos, I.P., Tsao, B.P., Tschan, M.P., Tse, H.-F., Tse, T.F., Tsugawa, H., Tsvetkov, A.S., Tumbarello, D.A., Tumtas, Y., Tuñón, M.J., Turcotte, S., Turk, B., Turk, V., Turner, B.J., Tuxworth, R.I., Tyler, J.K., Tyutereva, E.V., Uchiyama, Y., Ugun-Klusek, A., Uhlig, H.H., Ułamek-Kozioł, M., Ulasov, I.V., Umekawa, M., Ungermann, C., Unno, R., Urbe, S., Uribe-Carretero, E., Üstün, S., Uversky, V.N., Vaccari, T., Vaccaro, M.I., Vahsen, B.F., Vakifahmetoglu-Norberg, H., Valdor, R., Valente, M.J., Valko, A., Vallee, R.B., Valverde, A.M., Van Den Berghe, G., Van Der Veen, S., Van Kaer, L., Van Loosdregt, J., Van Wijk, S.J.L., Vandenberghe, W., Vanhorebeek, I., Vannier-Santos, M.A., Vannini, N., Vanrell, M.C., Vantaggiato, C., Varano, G., Varela-Nieto, I., Varga, M., Vasconcelos, M.H., Vats, S., Vavvas, D.G., Vega-Naredo, I., Vega-Rubin-de-Celis, S., Velasco, G., Velázquez, A.P., Vellai, T., Vellenga, E., Velotti, F., Verdier, M., Verginis, P., Vergne, I., Verkade, P., Verma, M., Verstreken, P., Vervliet, T., Vervoorts, J., Vessoni, A.T., Victor, V.M., Vidal, M., Vidoni, C., Vieira, O.V., Vierstra, R.D., Viganó, S., Vihinen, H., Vijayan, V., Vila, M., Vilar, M., Villalba, J.M., Villalobo, A., Villarejo-Zori, B., Villarroya, F., Villarroya, J., Vincent, O., Vindis, C., Viret, C., Viscomi, M.T., Visnjic, D., Vitale, I., Vocadlo, D.J., Voitsekhovskaja, O.V., Volonté, C., Volta, M., Vomero, M., Von Haefen, C., Vooijs, M.A., Voos, W., Vucicevic, L., Wade-Martins, R., Waguri, S., Waite, K.A., Wakatsuki, S., Walker, D.W., Walker, M.J., Walker, S.A., Walter, J., Wandosell, F.G., Wang, B., Wang, Chao-Yung, Wang, Chen, Wang, Chenran, Wang, Chenwei, Wang, Cun-Yu, Wang, D., Wang, Fangyang, Wang, Feng, Wang, Fengming, Wang, G., Wang, Han, Wang, Hao, Wang, Hexiang, Wang, H.-G., Wang, Jianrong, Wang, Jigang, Wang, Jiou, Wang, Jundong, Wang, K., Wang, Lianrong, Wang, Liming, Wang, M.H., Wang, M., Wang, N., Wang, Pengwei, Wang, Peipei, Wang, Ping, Wang, Ping, Wang, Q.J., Wang, Q., Wang, Q.K., Wang, Q.A., Wang, W.-T., Wang, W., Wang, Xinnan, Wang, Xuejun, Wang, Yan, Wang, Yanchang, Wang, Yanzhuang, Wang, Y.-Y., Wang, Yihua, Wang, Yipeng, Wang, Yu, Wang, Yuqi, Wang, Zhe, Wang, Zhenyu, Wang, Zhouguang, Warnes,

G., Warnsmann, V., Watada, H., Watanabe, E., Watchon, M., Wawrzyńska, A., Weaver, T.E., Wegrzyn, G., Wehman, A.M., Wei, H., Wei, L., Wei, T., Wei, Y., Weiergräber, O.H., Weihl, C.C., Weindl, G., Weiskirchen, R., Wells, A., Wen, R.H., Wen, X., Werner, A., Weykopf, B., Wheatley, S.P., Whitton, J.L., Whitworth, A.J., Wiktorska, K., Wildenberg, M.E., Wileman, T., Wilkinson, S., Willbold, D., Williams, B., Williams, R.S.B., Williams, R.L., Williamson, P.R., Wilson, R.A., Winner, B., Winsor, N.J., Witkin, S.S., Wodrich, H., Woehlbier, U., Wollert, T., Wong, E., Wong, J.H., Wong, R.W., Wong, V.K.W., Wong, W.W.-L., Wu, A.-G., Wu, C., Wu, Jian, Wu, Junfang, Wu, K.K., Wu, M., Wu, Shan-Ying, Wu, Shengzhou, Wu, Shu-Yan, Wu, Shufang, Wu, W.K.K., Wu, Xiaohong, Wu, Xiaoqing, Wu, Y.-W., Wu, Y., Xavier, R.J., Xia, H., Xia, L., Xia, Z., Xiang, G., Xiang, J., Xiang, M., Xiang, W., Xiao, B., Xiao, G., Xiao, Hengyi, Xiao, Hong-tao, Xiao, J., Xiao, L., Xiao, S., Xiao, Y., Xie, B., Xie, C.-M., Xie, M., Xie, Y., Xie, Zhiping, Xie, Zhonglin, Xilouri, M., Xu, C., Xu, E., Xu, H., Xu, Jing, Xu, JinRong, Xu, L., Xu, W.W., Xu, X., Xue, Y., Yakhine-Diop, S.M.S., Yamaguchi, M., Yamaguchi, O., Yamamoto, A., Yamashina, S., Yan, S., Yan, S.-J., Yan, Z., Yanagi, Y., Yang, C., Yang, D.-S., Yang, Huan, Yang, H.-T., Yang, Hui, Yang, J.-M., Yang, Jing, Yang, Jingyu, Yang, Ling, Yang, Liu, Yang, M., Yang, P.-M., Yang, Q., Yang, Seungwon, Yang, Shu, Yang, S.-F., Yang, W., Yang, W.Y., Yang, Xiaoyong, Yang, Xuesong, Yang, Yi, Yang, Ying, Yao, H., Yao, S., Yao, X., Yao, Y.-G., Yao, Y.-M., Yasui, T., Yazdankhah, M., Yen, P.M., Yi, C., Yin, X.-M., Yin, Y., Yin, Zhangyuan, Yin, Ziyi, Ying, M., Ying, Z., Yip, C.K., Yiu, S.P.T., Yoo, Y.H., Yoshida, K., Yoshii, S.R., Yoshimori, T., Yousefi, B., Yu, B., Yu, H., Yu, J., Yu, J., Yu, L., Yu, M.-L., Yu, S.-W., Yu, V.C., Yu, W.H., Yu, Zhengping, Yu, Zhou, Yuan, J., Yuan, L.-Q., Yuan, S., Yuan, S.-S.F., Yuan, Y., Yuan, Z., Yue, J., Yue, Z., Yun, J., Yung, R.L., Zacks, D.N., Zaffagnini, G., Zambelli, V.O., Zanella, I., Zang, Q.S., Zanivan, S., Zappavigna, S., Zaragoza, P., Zarbalis, K.S., Zarebkohan, A., Zarrouk, A., Zeitlin, S.O., Zeng, Jialiu, Zeng, Ju-deng, Žerovnik, E., Zhan, L., Zhang, B., Zhang, D.D., Zhang, Hanlin, Zhang, Hong, Zhang, Hong, Zhang, Honghe, Zhang, Huafeng, Zhang, Huaye, Zhang, Hui, Zhang, H.-L., Zhang, Jianbin, Zhang, Jianhua, Zhang, J.-P., Zhang, K.Y.B., Zhang, L.W., Zhang, Lin, Zhang, Lisheng, Zhang, Lu, Zhang, Luoying, Zhang, M., Zhang, P., Zhang, S., Zhang, W., Zhang, Xiangnan, Zhang, X.-W., Zhang, Xiaolei, Zhang, Xiaoyan, Zhang, Xin, Zhang, Xinxin, Zhang, X.D., Zhang, Yang, Zhang, Yanjin, Zhang, Yi, Zhang, Y.-D., Zhang, Yingmei, Zhang, Y.-Y., Zhang, Yuchen, Zhang, Zhe, Zhang, Zhengguang, Zhang, Zhibing, Zhang, Zhihai, Zhang, Zhiyong, Zhang, Zili, Zhao, H., Zhao, L., Zhao, S., Zhao, T., Zhao, X.-F., Zhao, Ying, Zhao, Yongchao, Zhao, Yongliang, Zhao, Yuting, Zheng, G., Zheng, K., Zheng, L., Zheng, S., Zheng, X.-L., Zheng, Y., Zheng, Z.-G., Zhivotovsky, B., Zhong, Q., Zhou, A., Zhou, B., Zhou, C., Zhou, G., Zhou, Hao, Zhou, Hong, Zhou, Hongbo, Zhou, Jie, Zhou, Jing, Zhou, Jing, Zhou, Jiyong, Zhou, K., Zhou, R., Zhou, X.-J., Zhou, Yanshuang, Zhou, Yinghong, Zhou, Yubin, Zhou, Z.-Y., Zhou, Z., Zhu, B., Zhu, C., Zhu, G.-Q., Zhu, Haining, Zhu, Hongxin, Zhu, Hua, Zhu, W.-G., Zhu, Yanping, Zhu, Yushan, Zhuang, H., Zhuang, X., Zientara-Rytter, K., Zimmermann, C.M., Ziviani, E., Zoladek, T., Zong, W.-X., Zorov, D.B., Zorzano, A., Zou, W., Zou, Zhen, Zou, Zhengzhi, Zuryn, S., Zwerschke, W., Brand-Saberi, B., Dong, X.C., Kenchappa, C.S., Li, Zuguo, Lin, Y., Oshima, S., Rong, Y., Sluimer, J.C., Stallings, C.L., Tong, C.-K., 2021. Guidelines for the use and interpretation of assays for monitoring autophagy (4th edition)[1]. Autophagy 17, 1–382. https://doi.org/10.1080/15548627.2020.1797280

Krause, M., Samolej, J., Yakimovich, A., Kriston-Vizi, J., Huttunen, M., Lara-Reyna, S., Frickel, E.-M., Mercer, J., 2024. Vaccinia virus subverts xenophagy through phosphorylation and nuclear targeting of p62. J. Cell Biol. 223, e202104129. https://doi.org/10.1083/jcb.202104129

Laliberte, J.P., Weisberg, A.S., Moss, B., 2011. The membrane fusion step of vaccinia virus entry is cooperatively mediated by multiple viral proteins and host cell components. PLoS Pathog. 7, e1002446. https://doi.org/10.1371/journal.ppat.1002446

Lansiaux, E., Jain, N., Laivacuma, S., Reinis, A., 2022. The virology of human monkeypox virus (hMPXV): A brief overview. Virus Res. 322, 198932. https://doi.org/10.1016/j.virusres.2022.198932

Luc Vincent, 2000. Granulometries and Opening Trees. Fundam. Informaticae 41, 57–90.

Luc Vincent, 1992. Morphological Area Opening and Closing for Grayscale Images. Proc NATO Shape Pict. Workshop 197–208. https://doi.org/10.1007/978-3-662-03039-4_13

Mercer, J., Helenius, A., 2008. Vaccinia virus uses macropinocytosis and apoptotic mimicry to enter host cells. Science 320, 531–535. https://doi.org/10.1126/science.1155164

Mercer, J., Traktman, P., 2003. Investigation of structural and functional motifs within the vaccinia virus A14 phosphoprotein, an essential component of the virion membrane. J. Virol. 77, 8857–8871. https://doi.org/10.1128/jvi.77.16.8857-8871.2003

Mizushima, N., Noda, T., Yoshimori, T., Tanaka, Y., Ishii, T., George, M.D., Klionsky, D.J., Ohsumi, M., Ohsumi, Y., 1998. A protein conjugation system essential for autophagy. Nature 395, 395–398. https://doi.org/10.1038/26506

Moloughney, J.G., Monken, C.E., Tao, H., Zhang, H., Thomas, J.D., Lattime, E.C., Jin, S., 2011. Vaccinia virus leads to ATG12–ATG3 conjugation and deficiency in autophagosome formation. Autophagy 7, 1434–1447. https://doi.org/10.4161/auto.7.12.17793

Moss, B., 2024. Understanding the biology of monkeypox virus to prevent future outbreaks. Nat. Microbiol. 9, 1408–1416. https://doi.org/10.1038/s41564-024-01690-1

Moussatche, N., Condit, R.C., 2015. Fine structure of the vaccinia virion determined by controlled degradation and immunolocalization. Virology 475, 204–218. https://doi.org/10.1016/j.virol.2014.11.020

Nishida, Y., Arakawa, S., Fujitani, K., Yamaguchi, H., Mizuta, T., Kanaseki, T., Komatsu, M., Otsu, K., Tsujimoto, Y., Shimizu, S., 2009. Discovery of Atg5/Atg7-independent alternative macroautophagy. Nature 461, 654–658. https://doi.org/10.1038/nature08455

Niu, K., Fang, Y., Deng, Y., Wang, Z., Xie, S., Zhu, J., Song, B., Wu, W., Jing, Z., Peng, C., 2024. Poxvirus A52 is a host range factor for modified vaccinia virus Ankara (MVA) and promotes viral replication by disturbing the formation of autolysosomes. https://doi.org/10.1101/2024.06.13.598619

Ra, E.A., Lee, T.A., Won Kim, S., Park, A., Choi, H.J., Jang, I., Kang, S., Hee Cheon, J., Cho, J.W., Eun Lee, J., Lee, S., Park, B., 2016. TRIM31 promotes Atg5/Atg7-independent autophagy in intestinal cells. Nat. Commun. 7, 11726. https://doi.org/10.1038/ncomms11726

Rodríguez, J.R., Risco, C., Carrascosa, J.L., Esteban, M., Rodríguez, D., 1998. Vaccinia virus 15-kilodalton (A14L) protein is essential for assembly and attachment of viral crescents to virosomes. J. Virol. 72, 1287–1296. https://doi.org/10.1128/JVI.72.2.1287-1296.1998

Satheshkumar, P.S., Anton, L.C., Sanz, P., Moss, B., 2009. Inhibition of the ubiquitin-proteasome system prevents vaccinia virus DNA replication and expression of intermediate and late genes. J. Virol. 83, 2469–2479. https://doi.org/10.1128/JVI.01986-08

Schmidt, F.I., Bleck, C.K.E., Reh, L., Novy, K., Wollscheid, B., Helenius, A., Stahlberg, H., Mercer, J., 2013. Vaccinia virus entry is followed by core activation and proteasome-mediated release of the immunomodulatory effector VH1 from lateral bodies. Cell Rep. 4, 464–476. https://doi.org/10.1016/j.celrep.2013.06.028

Senkevich, T.G., Koonin, E.V., Moss, B., 2009. Predicted poxvirus FEN1-like nuclease required for homologous recombination, double-strand break repair and full-size genome formation. Proc. Natl. Acad. Sci. U. S. A. 106, 17921–17926. https://doi.org/10.1073/pnas.0909529106

Sheen, J.-H., Zoncu, R., Kim, D., Sabatini, D.M., 2011. Defective regulation of autophagy upon leucine deprivation reveals a targetable liability of human melanoma cells in vitro and in vivo. Cancer Cell 19, 613–628. https://doi.org/10.1016/j.ccr.2011.03.012

Tanida, I., Tanida-Miyake, E., Ueno, T., Kominami, E., 2001. The Human Homolog of Saccharomyces cerevisiae Apg7p Is a Protein-activating Enzyme for Multiple Substrates Including Human Apg12p, GATE-16, GABARAP, and MAP-LC3. J. Biol. Chem. 276, 1701–1706. https://doi.org/10.1074/jbc.C000752200

Tolonen, N., Doglio, L., Schleich, S., Krijnse Locker, J., 2001. Vaccinia virus DNA replication occurs in endoplasmic reticulum-enclosed cytoplasmic mini-nuclei. Mol. Biol. Cell 12, 2031–2046. https://doi.org/10.1091/mbc.12.7.2031

Townsley, A.C., Senkevich, T.G., Moss, B., 2005. The product of the vaccinia virus L5R gene is a fourth membrane protein encoded by all poxviruses that is required for cell entry and cell-cell fusion. J. Virol. 79, 10988–10998. https://doi.org/10.1128/JVI.79.17.10988-10998.2005

Valderrama, F., Cordeiro, J.V., Schleich, S., Frischknecht, F., Way, M., 2006. Vaccinia virus-induced cell motility requires F11L-mediated inhibition of RhoA signaling. Science 311, 377–381. https://doi.org/10.1126/science.1122411

Vargas, J.N.S., Hamasaki, M., Kawabata, T., Youle, R.J., Yoshimori, T., 2023. The mechanisms and roles of selective autophagy in mammals. Nat. Rev. Mol. Cell Biol. 24, 167–185. https://doi.org/10.1038/s41580-022-00542-2

Wang, A., Ren, J., Wang, C.P., Hascall, V.C., 2014. Heparin prevents intracellular hyaluronan synthesis and autophagy responses in hyperglycemic dividing mesangial cells and activates synthesis of an extensive extracellular monocyte-adhesive hyaluronan matrix after completing cell division. J. Biol. Chem. 289, 9418–9429. https://doi.org/10.1074/jbc.M113.541441

Zhang, H., Monken, C.E., Zhang, Y., Lenard, J., Mizushima, N., Lattime, E.C., Jin, S., 2006. Cellular autophagy machinery is not required for vaccinia virus replication and maturation. Autophagy 2, 91–95. https://doi.org/10.4161/auto.2.2.2297

A

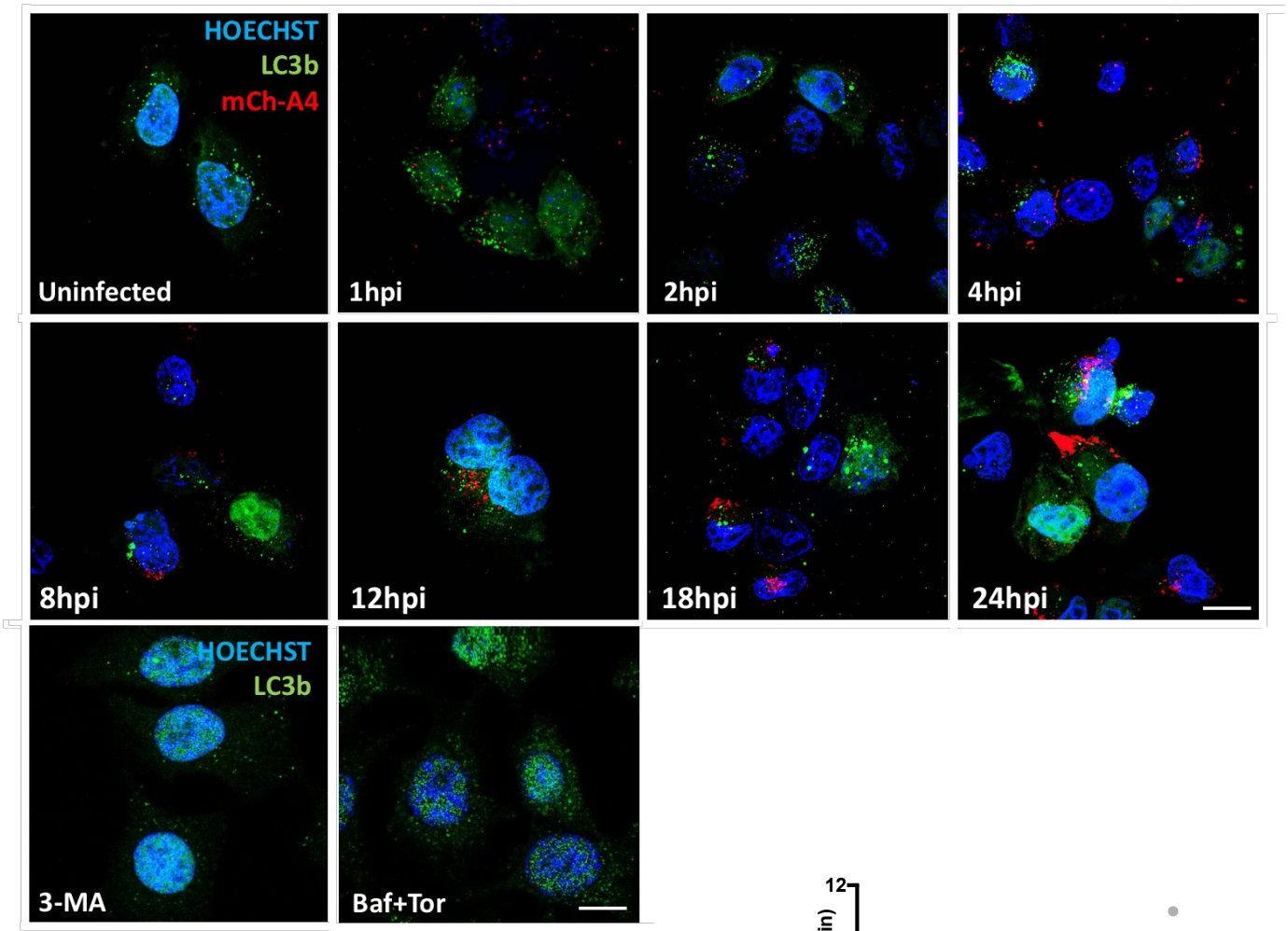
HOECHST
LC3b
mCh-A4
Uninfected
1hpi
2hpi
4hpi
8hpi
12hpi
18hpi
24hpi
HOECHST
LC3b
3-MA
Baf+Tor

B

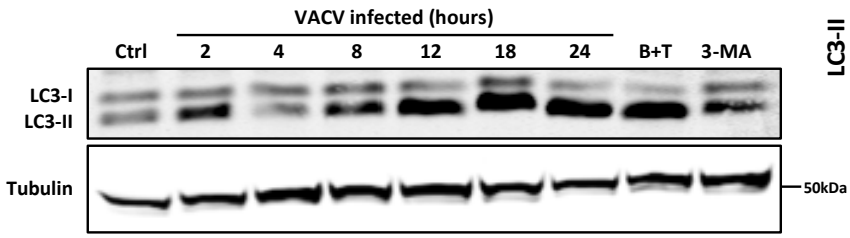
VACV infected (hours)
Ctrl
2
4
8
12
18
24
B+T
3-MA
LC3-I
LC3-II
Tubulin
50kDa

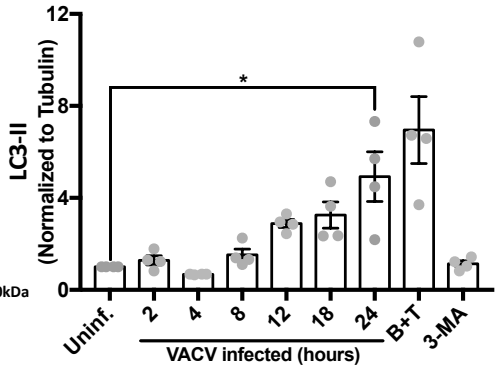
LC3-II
(Normalized to Tubulin)
12
8
4
0
*
Uninf.
2
4
8
12
18
24
B+T
3-MA
VACV infected (hours)

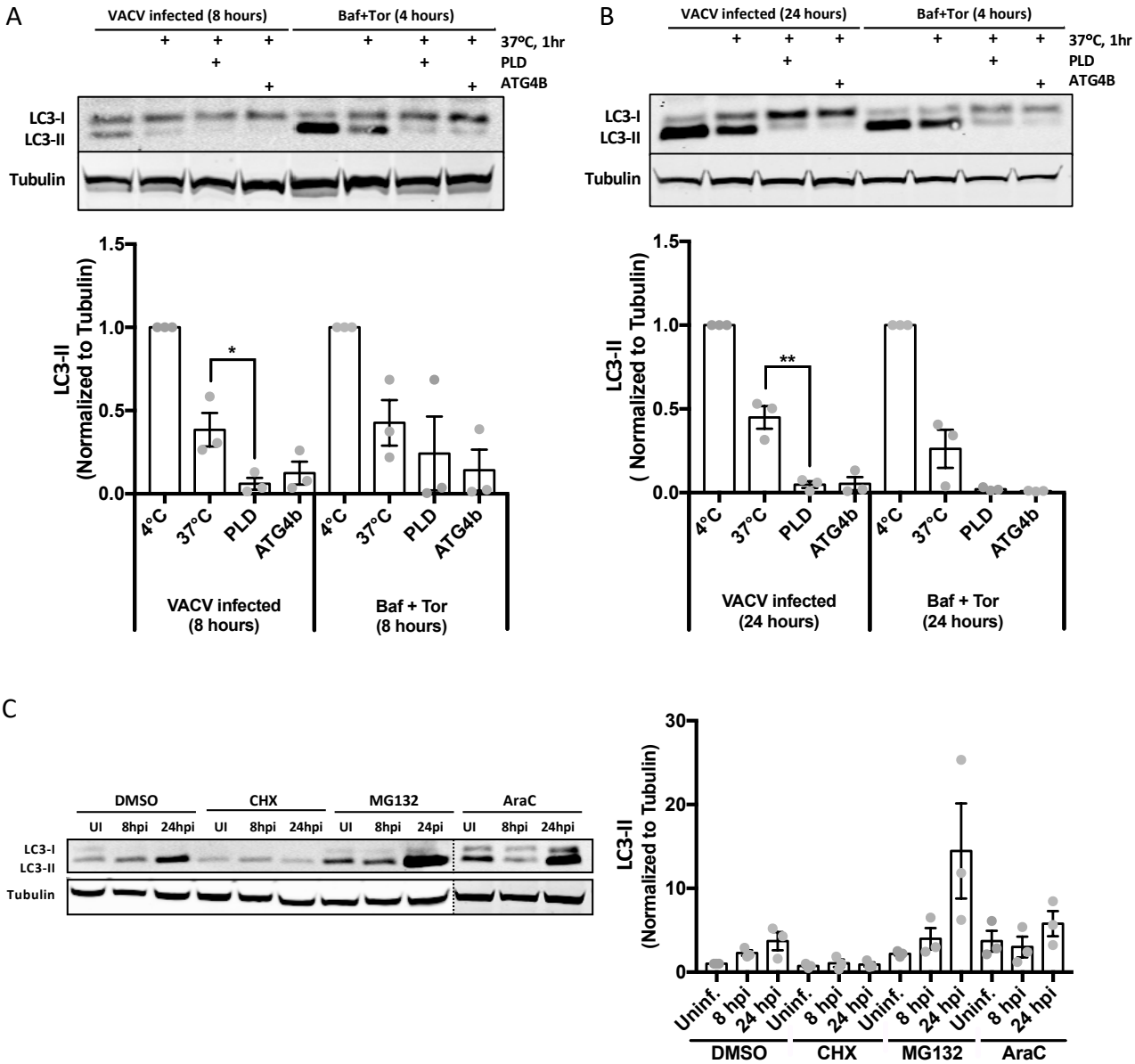

Krause et al., A granularity screening approach identifies candidate genes for VACV induced LC3 lipidation

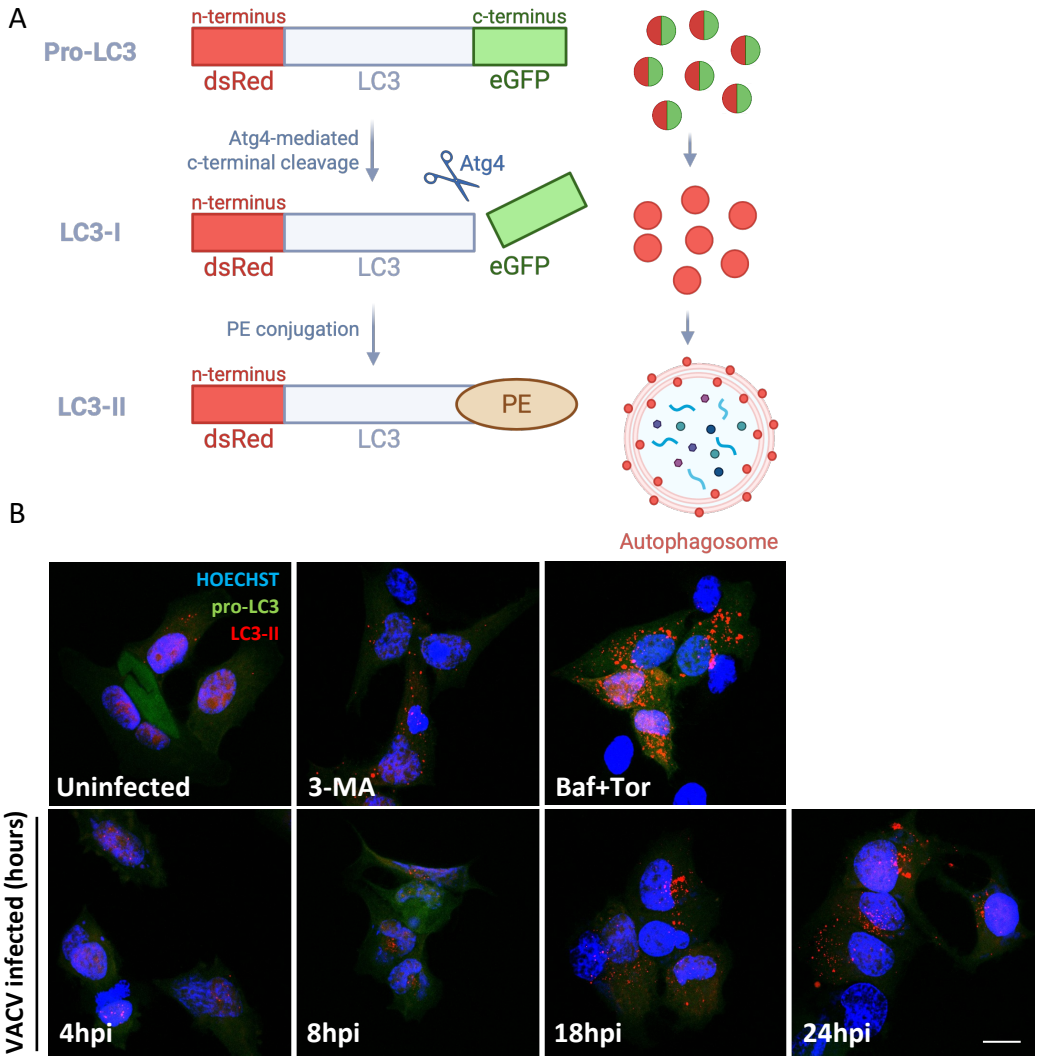

Krause et al., A granularity screening approach identifies candidate genes for VACV induced LC3 lipidation

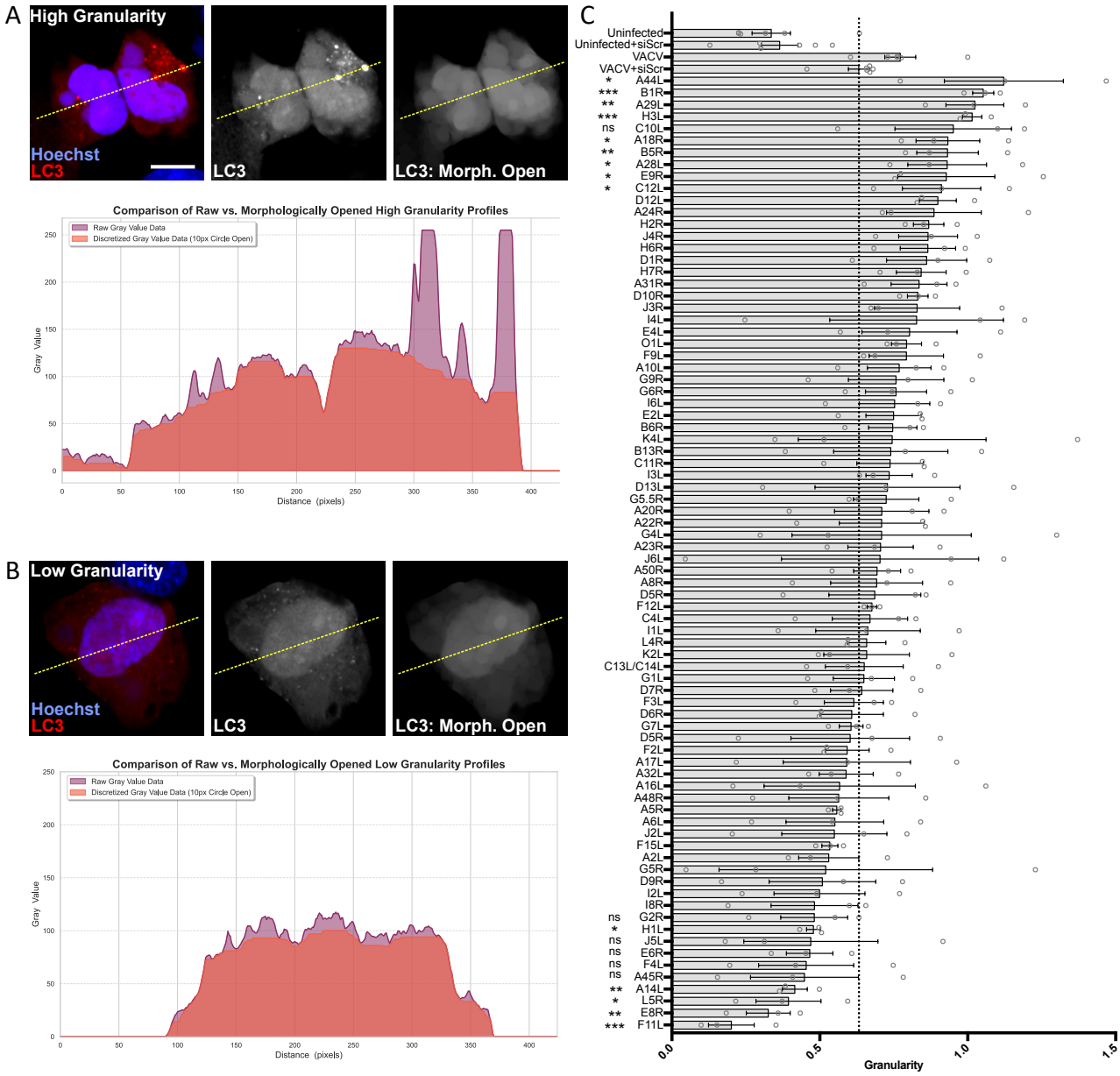

Krause et al., A granularity screening approach identifies candidate genes for VACV induced LC3 lipidation

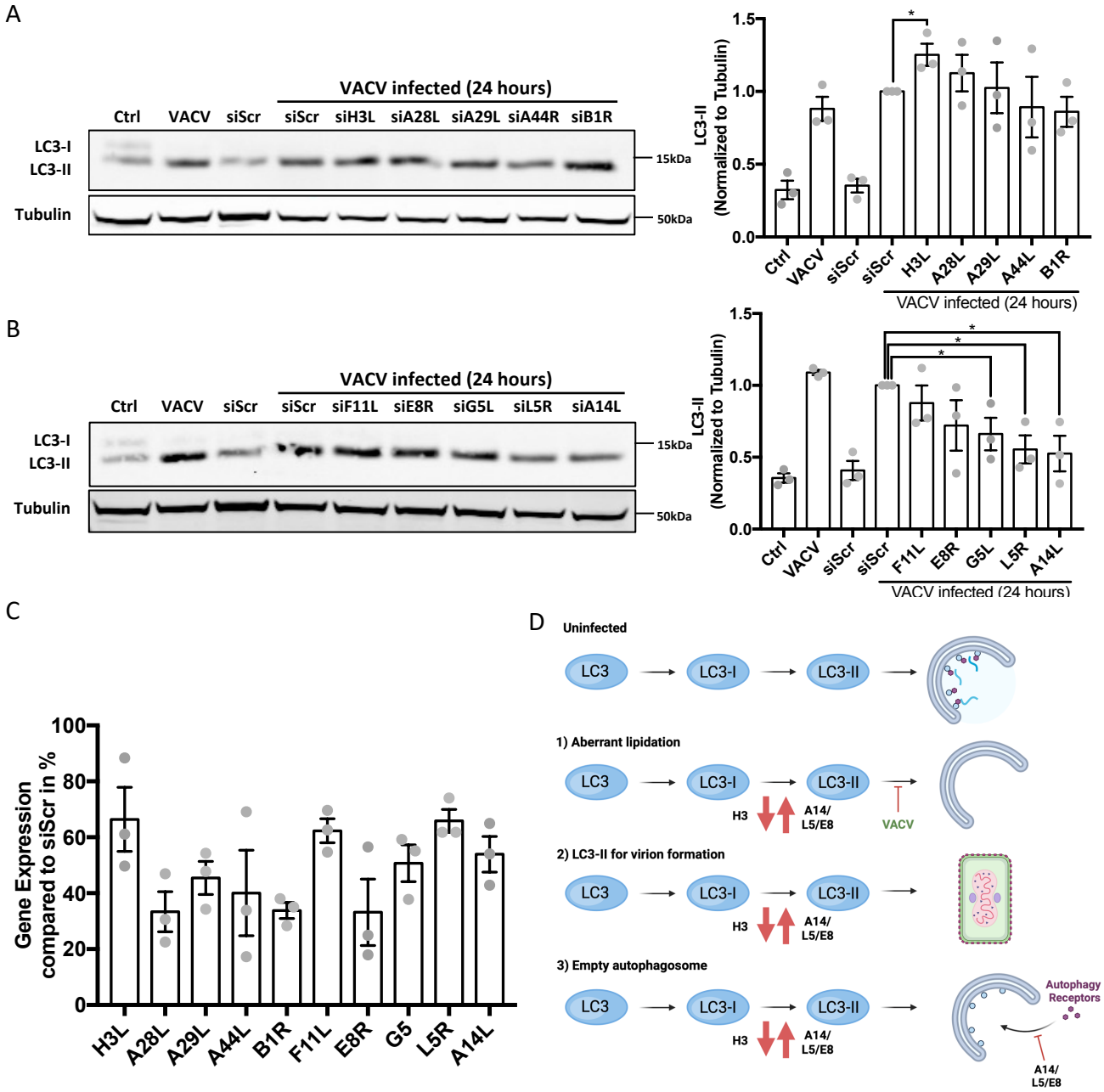

Krause et al., A granularity screening approach identifies candidate genes for VACV induced LC3 lipidation